Numerical Methods and Simulation Software for the Emission and Propagation of Fully- and Partially-Coherent Synchrotron Radiation Wavefronts

O. Chubar

NSLS-II Project, BNL, USA

Simulation Methods for X-ray Optical Systems, ESRF, February 24-25, 2009

Outline

- Introduction
  - Motivation
  - Existing Computer Codes
- Methods
  - Synchrotron Radiation:
    - Frequency Domain Electric Field from Liénard-Wiechert Potentials
  - Wavefront Propagation:
    - Kirchhoff Theorem for Single-Electron SR
    - Fourier Optics
- Computation Examples
  - Radiation from Insertion Devices:
    - Spectral Flux and Brightness
    - Intensity Distributions
    - Peculiarities of the Phase
  - Wavefront Propagation in THz to Hard X-Ray Spectral Range
- Possible Evolution

Motivation

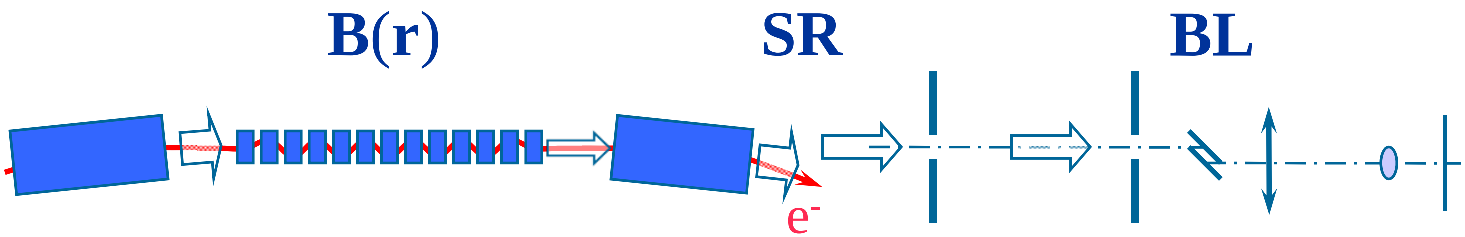

- Computation of **Magnetic Fields** produced by Permanent Magnets, Coils and Iron Blocks and in 3D space, optimized for the design of **Accelerator Magnets**, **Undulators** and **Wigglers**

RADIA

- Fast computation of **Synchrotron Radiation** emitted by relativistic electrons in Magnetic Field of arbitrary configuration
- **SR Wavefront Propagation** (Physical Optics)

SRW

Some Computer Codes

- For Synchrotron Radiation (Spontaneous Emission) and Wavefront Propagation Simulations
  - URGENT (R.Walker, ELETTRA)
  - XOP (S.Rio, ESRF, R.Dejus, APS)
  - WAVE + PHASE (J.Bahrdt, M.Scheer, BESSY)
  - SPECTRA (T.Tanaka, H.Kitamura, SPring-8)
  - SRW (O.Chubar, P.Elleaume, ESRF-SOLEIL, 1997-…)

Growing Importance of Physical Optics Calculations

Example: NSLS-II (operation to start in ~2015)

Approved Beamlines (December 2008)	Requires Physical Optics Simulations?
Inelastic Scattering Beamline (0.1 – 1 meV spectral resolution)	yes
Nanoprobe Beamline	yes
Coherent Hard X-ray Beamline	yes
Coherent Soft X-ray Beamline	yes
X-ray Absorption Spectroscopy Beamline	?
Powder Diffraction Beamline	yes

Spontaneous Emission by One Relativistic Electron Moving in Free Space

Lienard-Wiechert Potentials for One Electron: (Gaussian CGS)

$$\vec{A} = e\int_{-\infty}^{+\infty} \vec{\beta}_e R^{-1}\delta(\tau - t + R/c)\,d\tau, \quad \varphi = e\int_{-\infty}^{+\infty} R^{-1}\delta(\tau - t + R/c)\,d\tau$$

$$\Downarrow$$

Electric Field in Frequency Domain (exact expression!!!):

$$\vec{E}_\omega = \frac{ie\omega}{c}\int_{-\infty}^{+\infty} R^{-1}[\vec{\beta}_e - [1 + ic/(\omega R)]\,\vec{n}\,]\exp[i\omega(\tau + R/c)]\,d\tau \quad (\surd)$$

I.M.Ternov used this approach in Far Field approximation

$$\vec{E}_\omega = \frac{e}{c}\int_{-\infty}^{+\infty} \frac{\vec{n}\times\left[\left(\vec{n}-\vec{\beta}_e\right)\times\dot{\vec{\beta}}_e\right] + cR^{-1}\gamma^{-2}\left(\vec{n}-\vec{\beta}_e\right)}{R\cdot\left(1-\vec{n}\cdot\vec{\beta}_e\right)^2}\cdot\exp\left[i\omega\left(\tau + R/c\right)\right]d\tau$$

J.D.Jackson

Equivalence of the two expressions can be shown by integration by parts

Spontaneous Emission by One Relativistic Electron

Electric Field in Frequency Domain:

$$\vec{E}_\omega = \frac{ie\omega}{c}\int_{-\infty}^{+\infty} R^{-1}[\vec{\beta}_e - [1 + ic/(\omega R)]\,\vec{n}]\exp[i\omega(\tau + R/c)]d\tau$$

$$\vec{n} = \vec{R}/R,\ n_x \approx \frac{x - x_e}{z - c\tau},\ n_y \approx \frac{y - y_e}{z - c\tau}$$

Phase Expansion (valid in the Near- and in the Far Field):

$$\omega\cdot(\tau + R/c) \approx \Phi_0 + \frac{k}{2}\left[c\tau\gamma^{-2} + c\int_0^{\tau}|\vec{\beta}_{e\perp}|^2\,d\tilde{\tau} + \frac{|\vec{r}_\perp - \vec{r}_{e\perp}|^2}{z - c\tau}\right]$$

Asymptotic Expansion to accelerate computation and “improve” numerical convergence:

$$\int_{-\infty}^{+\infty} F\exp(i\Phi)ds = \int_{\tau_1}^{\tau_2} F\exp(i\Phi)ds + \int_{-\infty}^{\tau_1} F\exp(i\Phi)ds + \int_{\tau_2}^{+\infty} F\exp(i\Phi)ds$$

$$\int_{-\infty}^{\tau_1} F\exp(i\Phi)ds + \int_{\tau_2}^{+\infty} F\exp(i\Phi)ds \approx \left[\left(\frac{F}{i\Phi'} + \frac{F'\Phi' - F\Phi''}{\Phi'^3} + \ldots\right)\exp(i\Phi)\right]_{\tau_2}^{\tau_1}$$

Incoherent and Coherent Emission by Many Electrons

Electron Dynamics:

$$\begin{pmatrix} x_e \\ y_e \\ z_e \\ \beta_{xe} \\ \beta_{ye} \\ \delta\gamma_e \end{pmatrix} = \mathbf{A}(\tau) \begin{pmatrix} x_{e0} \\ y_{e0} \\ z_{e0} \\ x'_{e0} \\ y'_{e0} \\ \delta\gamma_{e0} \end{pmatrix} + \mathbf{B}(\tau)$$

← Initial Conditions

Spectral **Photon Flux per unit Surface** emitted by the **whole Electron Beam**:

$$\frac{dN_{ph}}{dtdS(d\omega/\omega)} = \frac{c^2 \alpha I}{4\pi^2 e^3} \left\langle \left| \vec{E}_\omega \right|^2 \right\rangle$$

"Incoherent" SR

↓

$$\left\langle \left| \vec{E}_\omega \right|^2 \right\rangle = \int \left| \vec{E}_{\omega 0}(\vec{r}; x_{e0}, y_{e0}, z_{e0}, x'_{e0}, y'_{e0}, \delta\gamma_{e0}) \right|^2 f(x_{e0}, y_{e0}, z_{e0}, x'_{e0}, y'_{e0}, \delta\gamma_{e0}) dx_{e0} dy_{e0} dz_{e0} dx'_{e0} dy'_{e0} d\delta\gamma_{e0} +$$

$$+ (N_e - 1) \left| \int \vec{E}_{\omega 0}(\vec{r}; x_{e0}, y_{e0}, z_{e0}, x'_{e0}, y'_{e0}, \delta\gamma_{e0}) f(x_{e0}, y_{e0}, z_{e0}, x'_{e0}, y'_{e0}, \delta\gamma_{e0}) dx_{e0} dy_{e0} dz_{e0} dx'_{e0} dy'_{e0} d\delta\gamma_{e0} \right|^2$$

↑

"Coherent" SR

Common Approximation for CSR: **"Thin" Electron Beam:** $\left\langle \left| \vec{E}_\omega \right|^2 \right\rangle_{CSR} \approx N_e \left| \int_{-\infty}^{\infty} \tilde{f}(z_{e0}) \exp(ikz_{e0}) dz_{e0} \right|^2 \left| \vec{E}_{\omega 1} \right|^2$

For Gaussian Longitudinal Bunch Profile: $\left\langle \left| \vec{E}_\omega \right|^2 \right\rangle_{CSR} \approx N_e \exp(-k^2 \sigma_b^2) \left| \vec{E}_{\omega 1} \right|^2$

However, if $f(x_{e0}, y_{e0}, z_{e0}, x'_{e0}, y'_{e0}, \delta\gamma_{e0})$ is Gaussian, the 6-fold integration can be done **analytically** (!)

$\Rightarrow$ Efficient method for CSR computation taking into account 6D phase space distribution of electrons

Self-Amplified Spontaneous Emission Described by Paraxial FEL Equations

Approximation of Slowly Varying Amplitude of Radiation Field

Particles' dynamics in undulator and radiation fields (averaged over many periods):

$$\frac{d\theta}{dz} = k_u - k_r \frac{1 + p_\perp^2 + a_u^2 - 2a_r a_u \cos(\theta + \phi_r)}{2\gamma^2}$$

$$\frac{d\gamma}{dz} = -\frac{k_r f_c a_r a_u}{\gamma} \sin(\theta + \phi_r)$$

$$\frac{d\vec{p}_\perp}{dz} = -\frac{1}{2\gamma} \frac{\partial a_u^2}{\partial \vec{r}_\perp} + \mathbf{k}_{foc} \vec{r}_\perp$$

$$\frac{d\vec{r}_\perp}{dz} = \frac{\vec{p}_\perp}{\gamma}$$

W.B.Colson
J.B.Murphy
C.Pellegrini
E.Saldin
E.Bessonov
et. al.

Paraxial wave equation with current:

$$\left[2ik_r \frac{\partial}{\partial z} + \nabla_\perp^2\right] a_r \exp(i\phi_r) = -\frac{e\varepsilon_0 I f_c a_u}{mc} \left\langle \frac{\exp(-i\theta)}{\gamma} \right\rangle$$

Solving this system gives Electric Field at the FEL exit for one "Slice": $E_{slice}\big|_{z=z_{exit}} \sim a_r \exp(i\phi_r)\big|_{z=z_{exit}}$

Loop on "Slices" (copying Electric Field to a next slice from previous slice, starting from back)

Time- (and Frequency-) Domain Electric Field in transverse plane at FEL exit: $E(x, y, z_{exit}, t) \leftrightarrow E_\omega(x, y, z_{exit})$

- Popular TD 3D FEL computer code: **GENESIS** (S.Reiche)
  Integrated to SRW on C++ level

Wavefront Propagation:
Case of Full Transverse Coherence

Kirchhoff Integral Theorem applied to Spontaneous Emission by One Electron

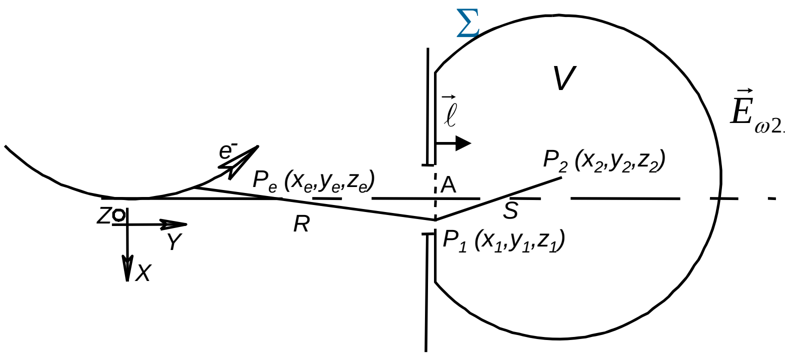

$$\vec{E}_{\omega 2\perp}(P_2) \approx \frac{k^2 e}{4\pi}\int_{-\infty}^{+\infty} d\tau \iint_A \frac{\vec{\beta}_{e\perp} - \vec{n}_\perp}{RS} \exp[ik(c\tau + R + S)] \cdot (\vec{\ell}\cdot\vec{n}_{p_e p_1} + \vec{\ell}\cdot\vec{n}_{p_1 p_2}) d\Sigma$$

$$k = \omega/c$$

Valid at large observation angles;
Is applicable to complicated cases of diffraction inside vacuum chamber

Huygens-Fresnel Principle

$$\vec{E}_{\omega 2\perp}(P_2) \approx \frac{k}{4\pi i}\iint_A \vec{E}_{\omega 1\perp}(P_1)\frac{\exp(ikS)}{S}(\vec{\ell}\cdot\tilde{\vec{n}} + \vec{\ell}\cdot\vec{n}_{p_1 p_2}) d\Sigma$$

Fourier Optics

Free Space:
(between parallel planes perpendicular to optical axis)

$$\vec{E}_{\omega 2\perp}(x_2,y_2) \approx \frac{k}{2\pi i L}\iint \vec{E}_{\omega 1\perp}(x_1,y_1)\exp[ik[L^2 + (x_2 - x_1)^2 + (y_2 - y_1)^2]^{1/2}]dx_1 dy_1$$

Assumption of small angles

"Thin" Optical Element:

$$\vec{E}_{\omega 2\perp}(x,y) \approx \mathbf{T}(x,y,\omega)\,\vec{E}_{\omega 1\perp}(x,y)$$

"Thick" Optical Element:
(from transverse plane before the element to a transverse plane immediately after it)

$$\vec{E}_{\omega 2\perp}(x_2,y_2) \approx \mathbf{G}(x_2,y_2,\omega)\exp[ik\Lambda(x_2,y_2,k)]\,\vec{E}_{\omega 1\perp}(x_1(x_2,y_2), y_1(x_2,y_2))$$

E.g. from Stationary Phase method

"Economic" Version of Free-Space Fourier-Optics Propagator

Huygens-Fresnel Principle:
(paraxial approximation)

$$\vec{E}_{\omega 2\perp}(\vec{r}_2) \approx \frac{k}{2\pi i} \iint_{\Sigma_1} \vec{E}_{\omega 1\perp}(\vec{r}_1) \frac{\exp[ik\,|\vec{r}_2 - \vec{r}_1|]}{|\vec{r}_2 - \vec{r}_1|} d\Sigma_1$$

$$|\vec{r}_2 - \vec{r}_1| = [L^2 + (x_2 - x_1)^2 + (y_2 - y_1)^2]^{1/2}$$

Analytical Treatment of Quadratic Phase Term:

Before Propagation:

$$\vec{E}_{\omega 1\perp}(x_1, y_1) = \vec{F}_{\omega 1}(x_1, y_1) \exp\left[ik\frac{(x_1 - x_0)^2}{2R_x} + ik\frac{(y_1 - y_0)^2}{2R_y} \right]$$

After Propagation:

$$\vec{E}_{\omega 2\perp}(x_2, y_2) \approx \frac{k}{2\pi i L} \exp(ikL) \iint_{\Sigma} \vec{F}_{\omega 1}(x_1, y_1) \exp\left[ik\frac{(x_1 - x_0)^2}{2R_x} + ik\frac{(y_1 - y_0)^2}{2R_y} + ik\frac{(x_2 - x_1)^2 + (y_2 - y_1)^2}{2L} \right] dx_1 dy_1$$

$$= \frac{k}{2\pi i L} \exp\left[ikL + ik\frac{(x_2 - x_0)^2}{2(R_x + L)} + ik\frac{(y_2 - y_0)^2}{2(R_y + L)} \right] \times$$

$$\times \iint_{\Sigma} \vec{F}_{\omega 1}(x_1, y_1) \exp\left[ik\frac{R_x + L}{2R_x L}\left(x_1 - \frac{R_x x_2 + L x_0}{R_x + L} \right)^2 + ik\frac{R_y + L}{2R_y L}\left(y_1 - \frac{R_y y_2 + L y_0}{R_y + L} \right)^2 \right] dx_1 dy_1$$

$$= \vec{F}_{\omega 2}(x_2, y_2) \exp\left[ik\frac{(x_2 - x_0)^2}{2(R_x + L)} + ik\frac{(y_2 - y_0)^2}{2(R_y + L)} \right]$$

Wavefront Propagation:
Taking Into Account Partial Coherence

Averaging of Propagated One-Electron Intensity
over Phase-Space Volume occupied by Electron Beam:

$$I_{\omega}(x,y) = \int I_{\omega 0}(x,y;x_{e0},y_{e0},x'_{e0},y'_{e0},\delta\gamma_{e0})\, f(x_{e0},y_{e0},x'_{e0},y'_{e0},\delta\gamma_{e0})\, dx_{e0}dy_{e0}dx'_{e0}dy'_{e0}d\delta\gamma_{e0}$$

Convolution is valid in many cases:
- projection geometry;
- focusing by a thin lens;
- diffraction on one slit (/pinhole);
- ...

$$I_{\omega}(x,y) \approx \int_{-\infty}^{+\infty}\int_{-\infty}^{+\infty} \tilde{I}_{\omega 0}(x-\tilde{x}_e, y-\tilde{y}_e)\,\tilde{f}(\tilde{x}_e,\tilde{y}_e)\, d\tilde{x}_e d\tilde{y}_e$$

OR:

Propagation of Mutual Intensity

Kwang-Je Kim

Mutual Intensity:

$$M_{\omega}(x,y;\tilde{x},\tilde{y}) = \int \vec{E}_{\omega 0\perp}(x,y;\ x_{e0},y_{e0},x'_{e0},y'_{e0},\delta\gamma_{e0})\vec{E}^{*}_{\omega 0\perp}(\tilde{x},\tilde{y};\ x_{e0},y_{e0},x'_{e0},y'_{e0},\delta\gamma_{e0})$$
$$\times f(x_{e0},y_{e0},x'_{e0},y'_{e0},\delta\gamma_{e0})\, dx_{e0}dy_{e0}dx'_{e0}dy'_{e0}d\delta\gamma_{e0}$$

Wigner Distribution (or mathematical Brightness):

$$B_{\omega}(x,y;\theta_x,\theta_y) = \frac{1}{2\pi}\int_{-\infty}^{+\infty}\int_{-\infty}^{+\infty} M_{\omega}(x,y;\tilde{x},\tilde{y})\exp[ik(\theta_x\tilde{x}+\theta_y\tilde{y})]d\tilde{x}d\tilde{y}$$

Examples: Undulator Radiation

On-Axis Spectrum (taking into account e-beam Emittance)

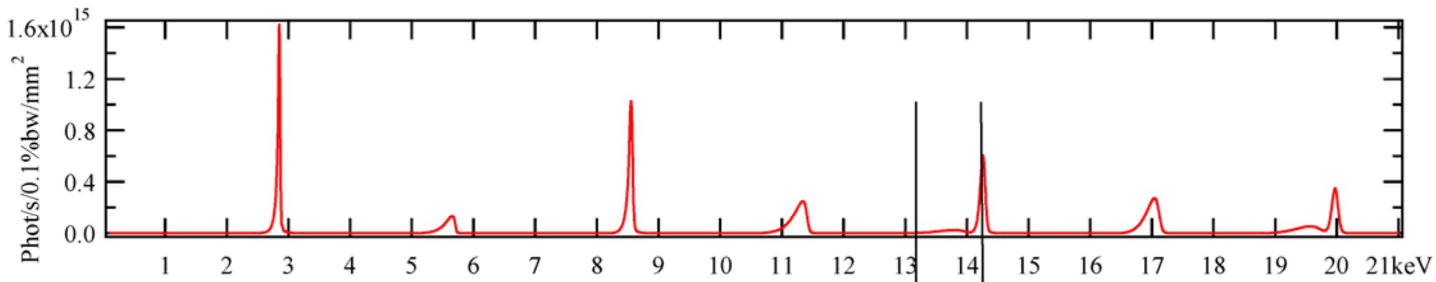

Undulator:

λ_u = 35 mm

K = 2.2

Spectral Flux / Surface

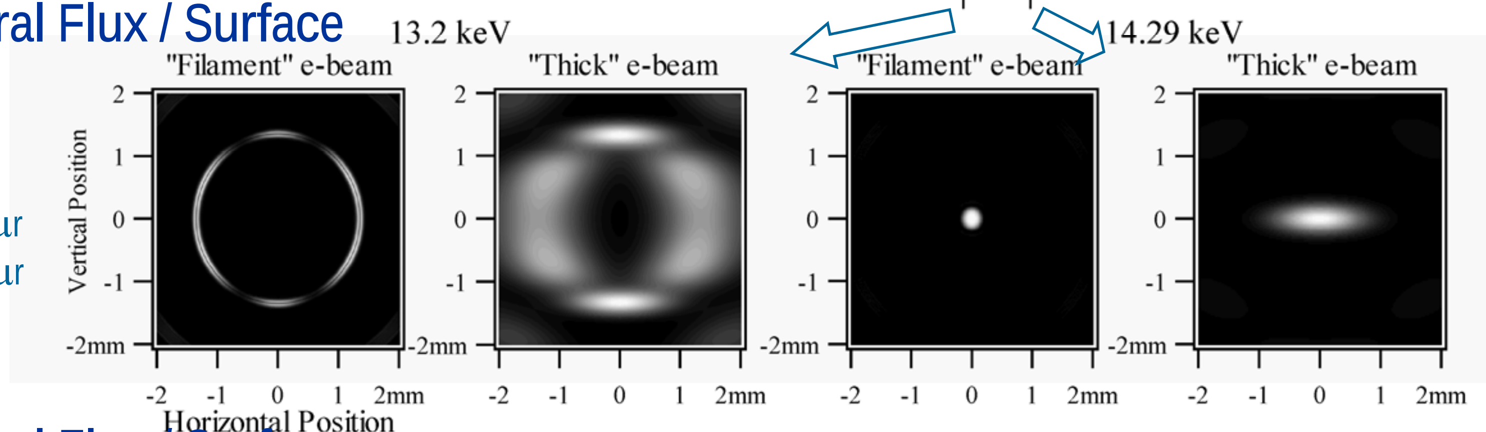

e-Beam:

E = 6 GeV

$\sigma_{x\,eff}\,/\,R$ = 16.2 μr

$\sigma_{z\,eff}\,/\,R$ = 3.96 μr

$\sigma_E\,/\,E = 10^{-3}$

R = 30 m

Spectral Flux / Surface (vertical cuts)

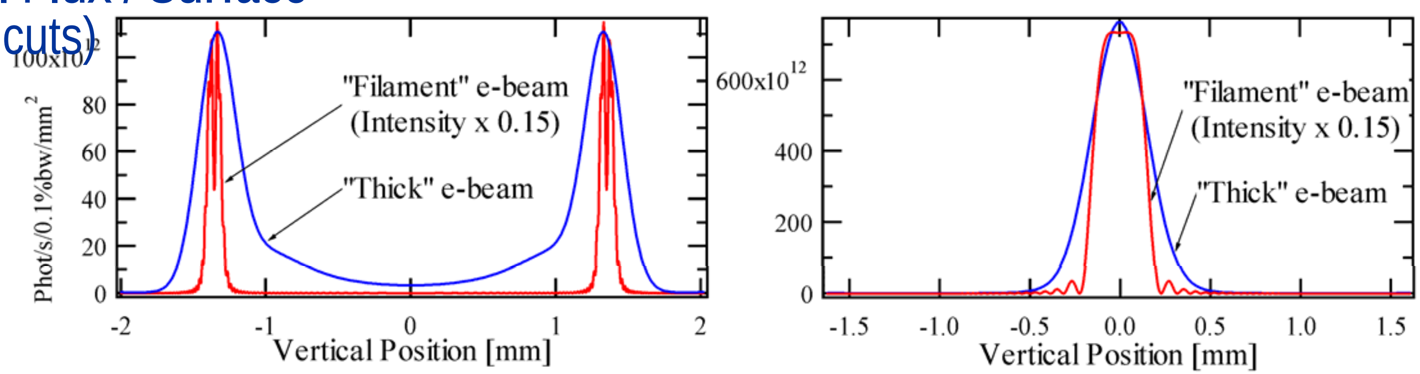

Examples: Undulator Radiation
U20 (SOLEIL) Spectra and Intensity Distributions @ H3

Spectral Flux

Spectral Flux / Surface (vertical cuts)

Spectral Flux / Surface @ 17.4 m

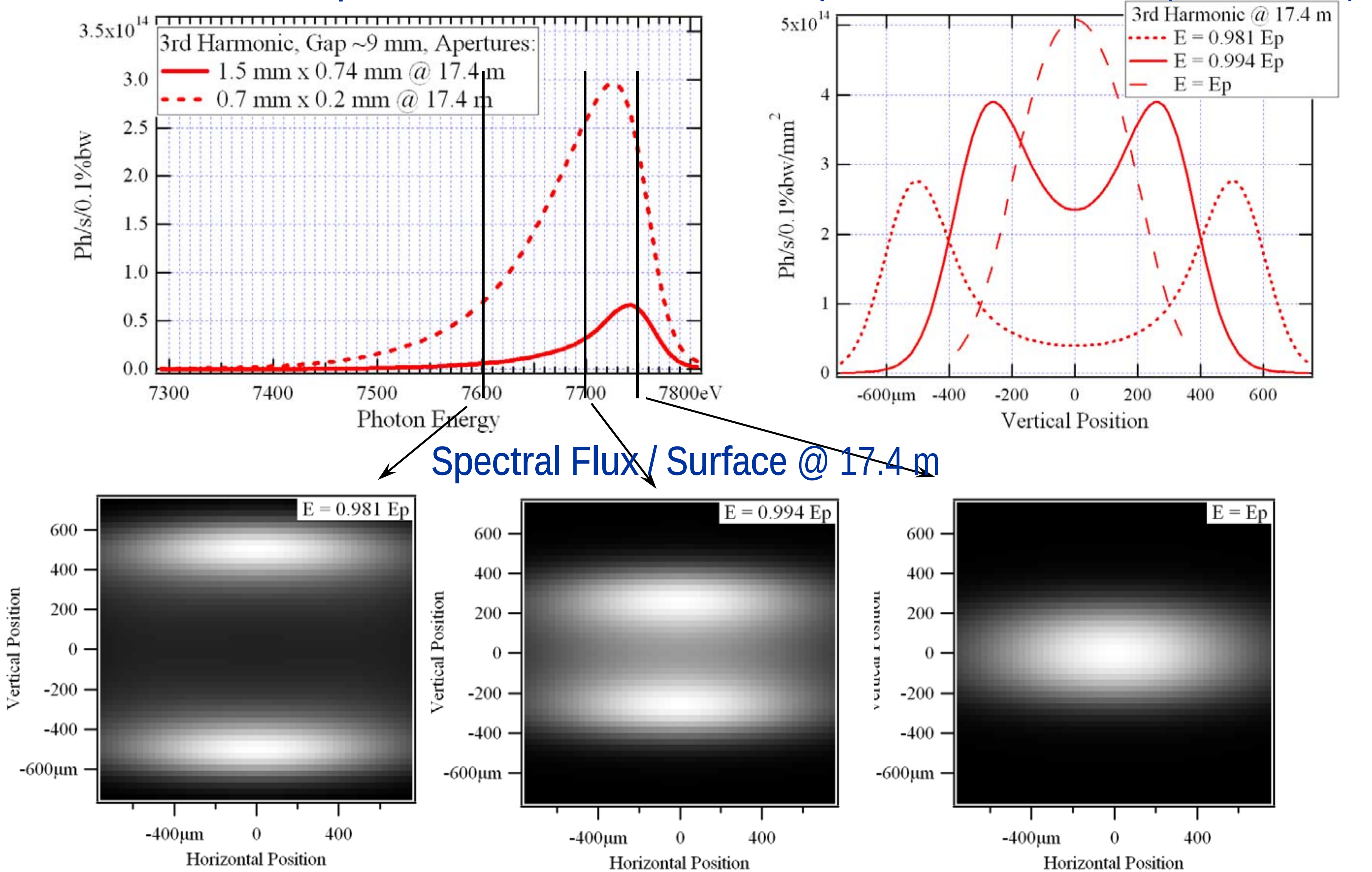

In-Vacuum Hybrid Undulator U20 (SWING)
Spectral Shimming Results

On-Axis Single-Electron Spectra Before and After Shimming (10 m from source)

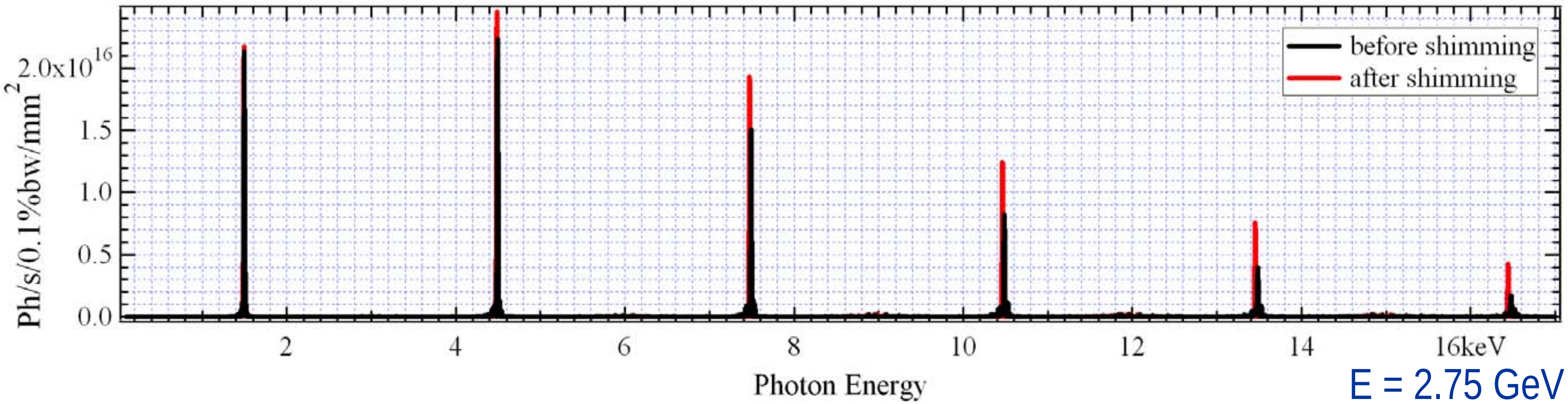

E = 2.75 GeV

Evolution of 11th Harmonic of Single-Electron Spectrum

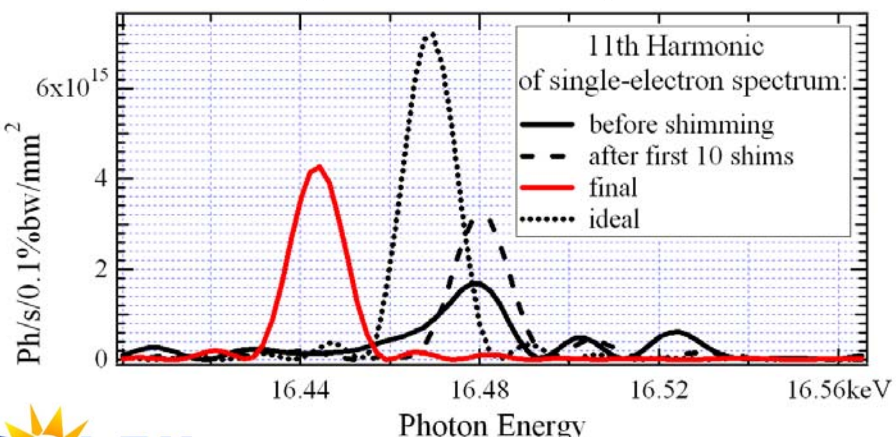

On-Axis Intensity Taking into account E-Beam Emittance and Energy Spread

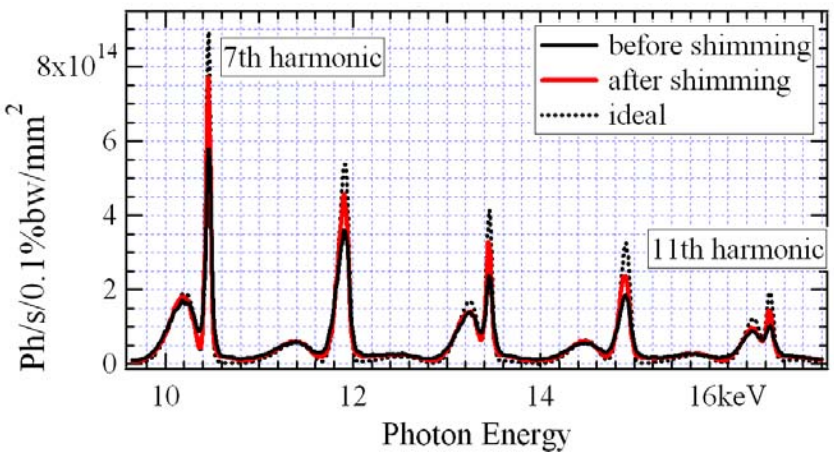

SOLEIL SYNCHROTRON

RMS Radiation Phase Error after Shimming ~2.5°

$\varepsilon_x = 3.7$ nm; $\sigma_E/E = 10^{-3}$

APPLE-II Undulator HU80-PLEIADES:
Quasi-Periodic Field, Trajectory, Spectra

Measured Vertical Magnetic Field

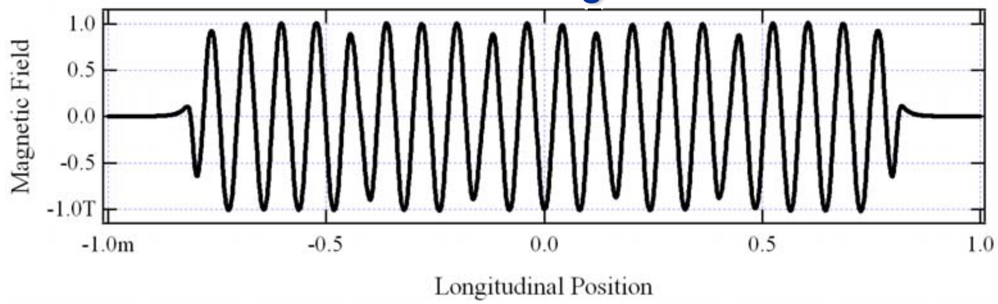

Horizontal Trajectory

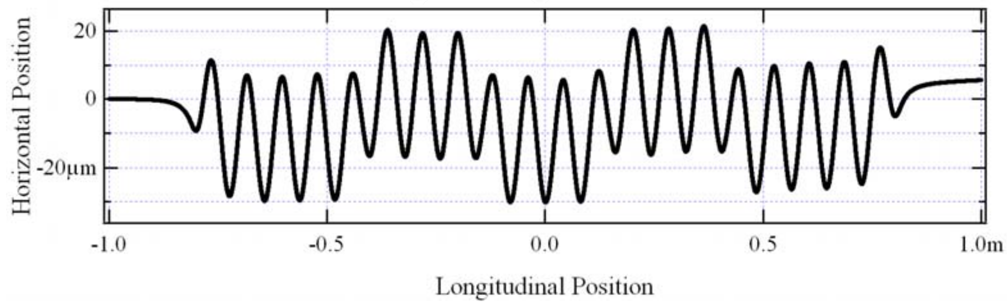

Quasi-Periodic Mode was realized by 11 mm displacement of some longitudinally-polarized magnet blocks

Spectra Through Finite Apertures

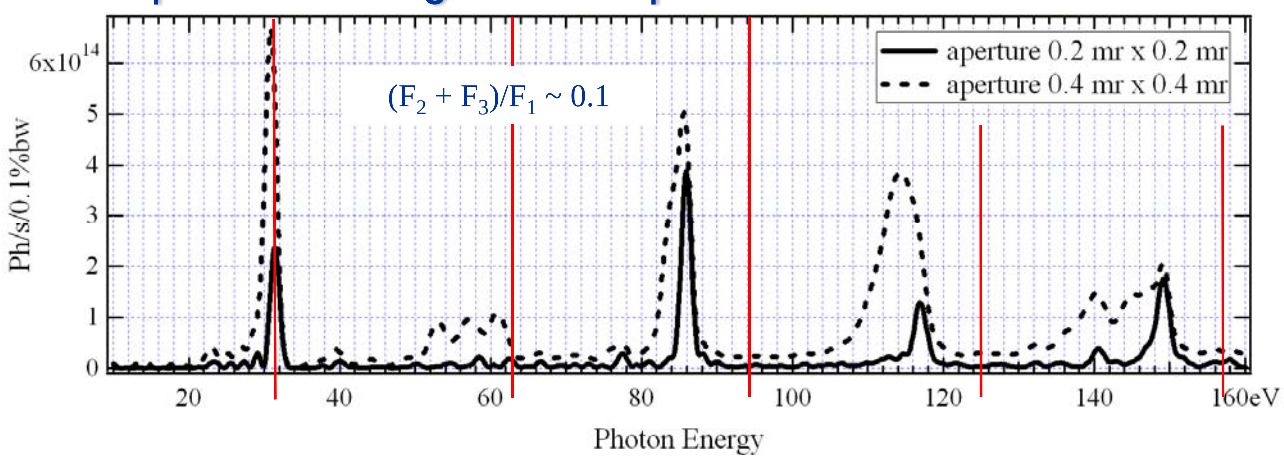

SOLEIL SYNCHROTRON

RADIA-SRW Examples:
Electromagnetic Elliptical Undulator HU256

The Structure (A.Dael, SOLEIL; P.Vobly, BINP)

RADIA Model

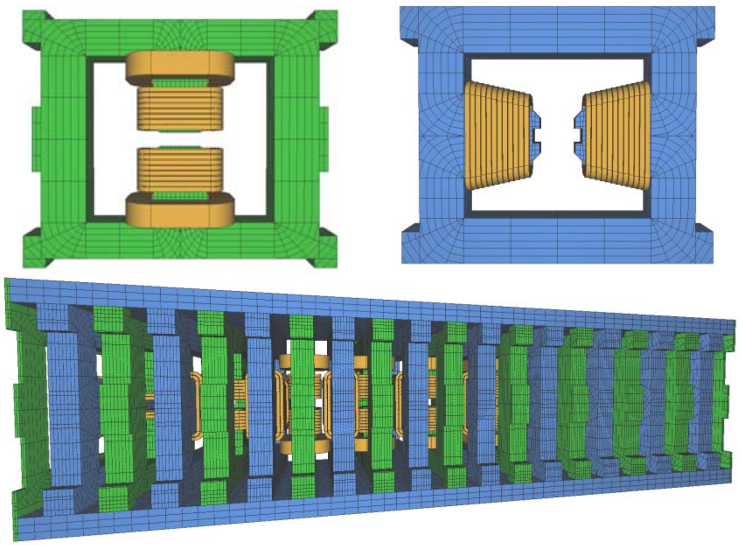

Magnetic Fields at Max. Currents (RADIA)

$I_{z\,max}$= 180 A, $I_{x\,max}$= 250 A

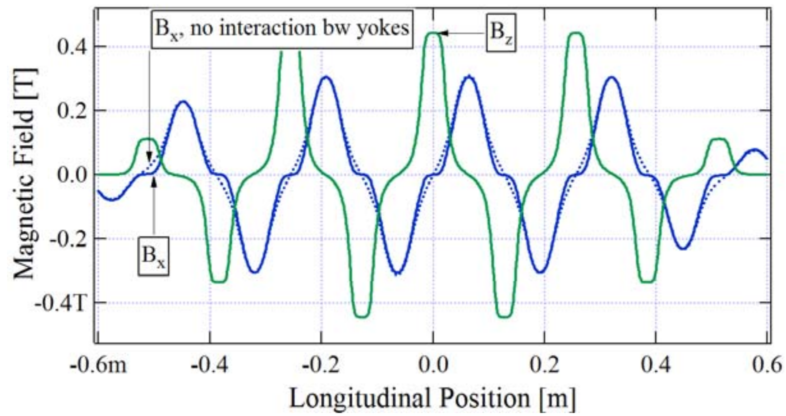

Calculated Spectra at Maximal Currents (SRW)

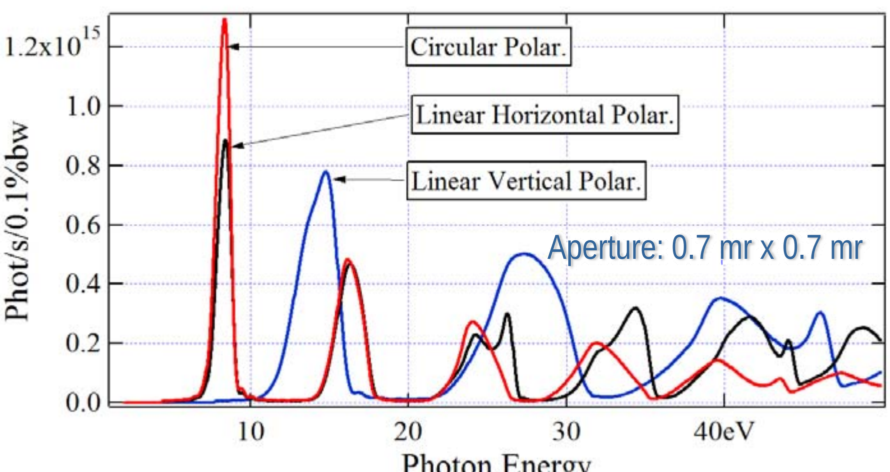

Specifications:

Circular Polarization: $\varepsilon_{1\,min}$ < 10 eV
Linear Horiz. Polarization: $\varepsilon_{1\,min}$ < 10 eV
Linear Vertical Polarization: $\varepsilon_{1\,min}$ < 20 eV

SOLEIL SYNCHROTRON

Examples: Undulator Radiation
Maximal Spectral Flux at Various Polarizations

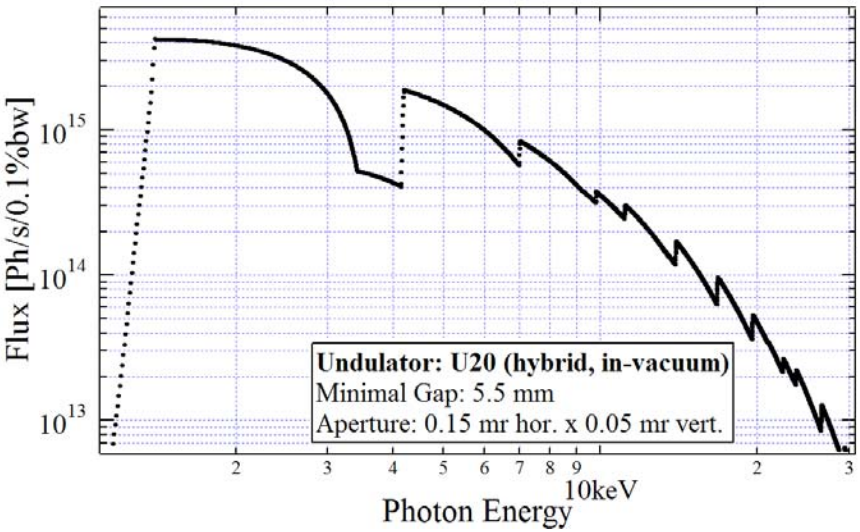

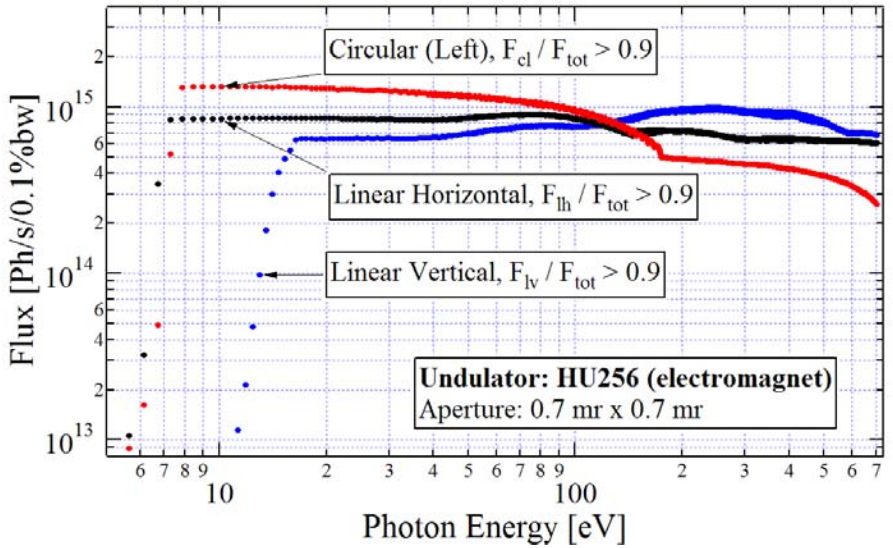

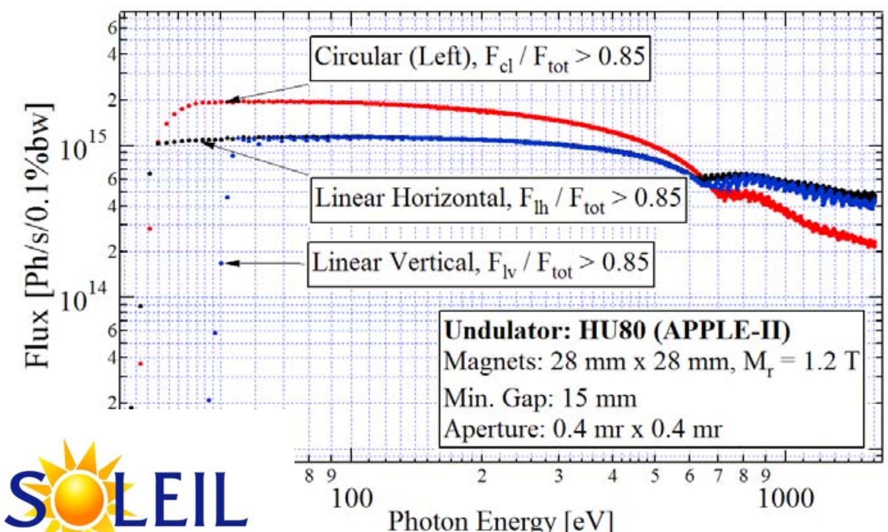

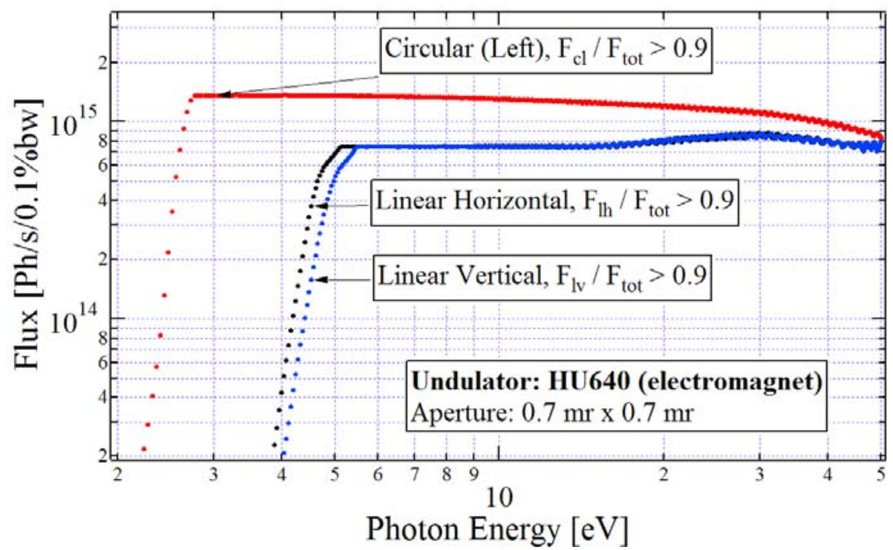

SOLEIL SYNCHROTRON

Examples: Wavefront Propagation

Focusing of Undulator Radiation

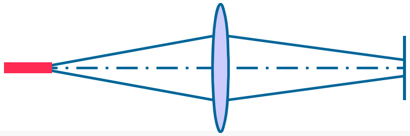

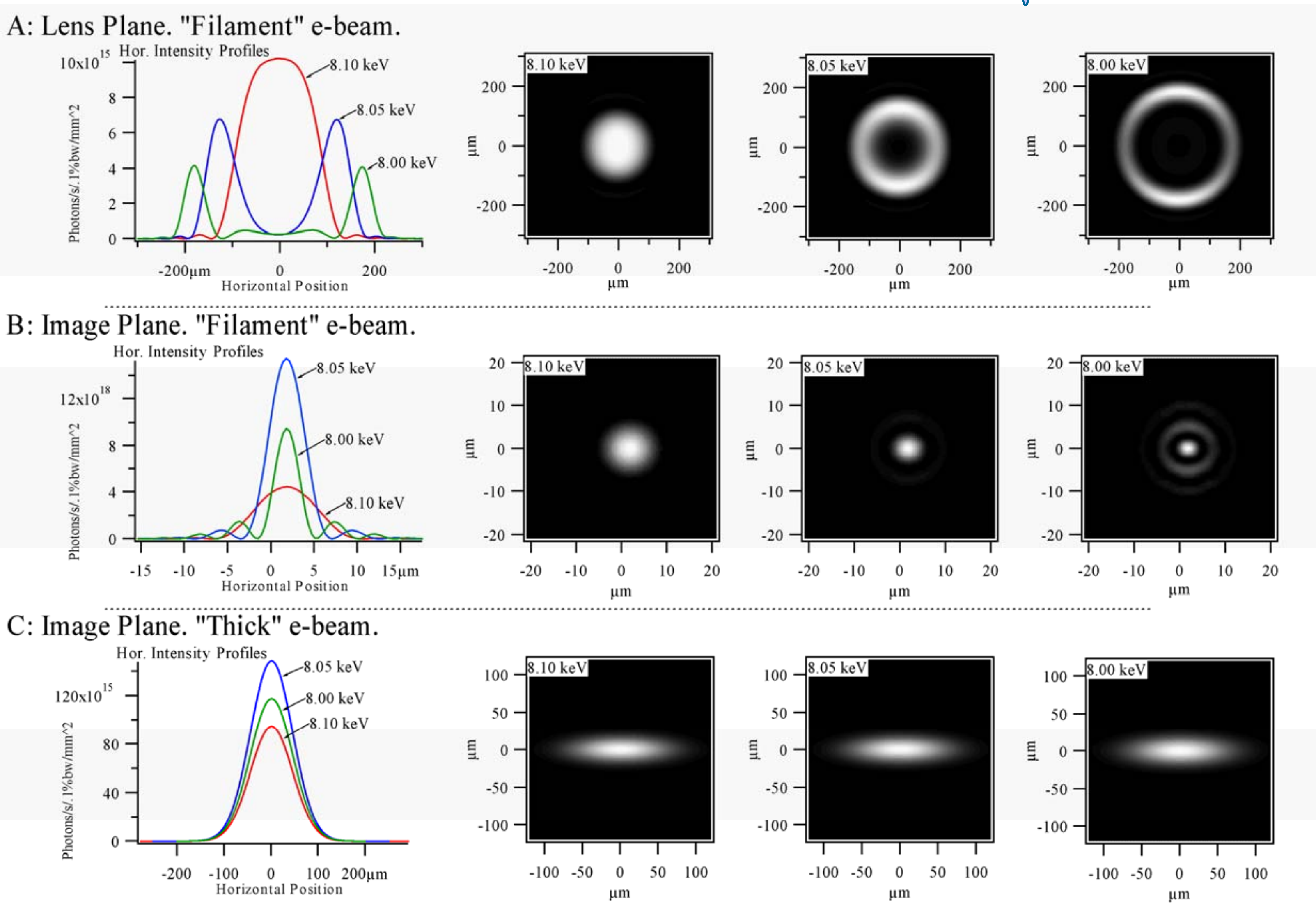

Examples: Wavefront Propagation

Peculiarities of UR Wavefronts

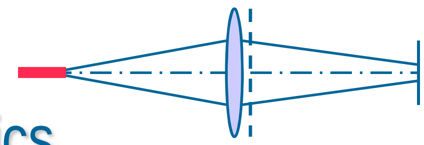

Planar Undulator, Odd Harmonics

E = 6 GeV; *K* = 2.2; 38 x 42 mm; ε = 2.36 keV (~ fundamental)

1 : 1 imaging; 30 m from middle of Undulator to Thin Lens & Phase Correction

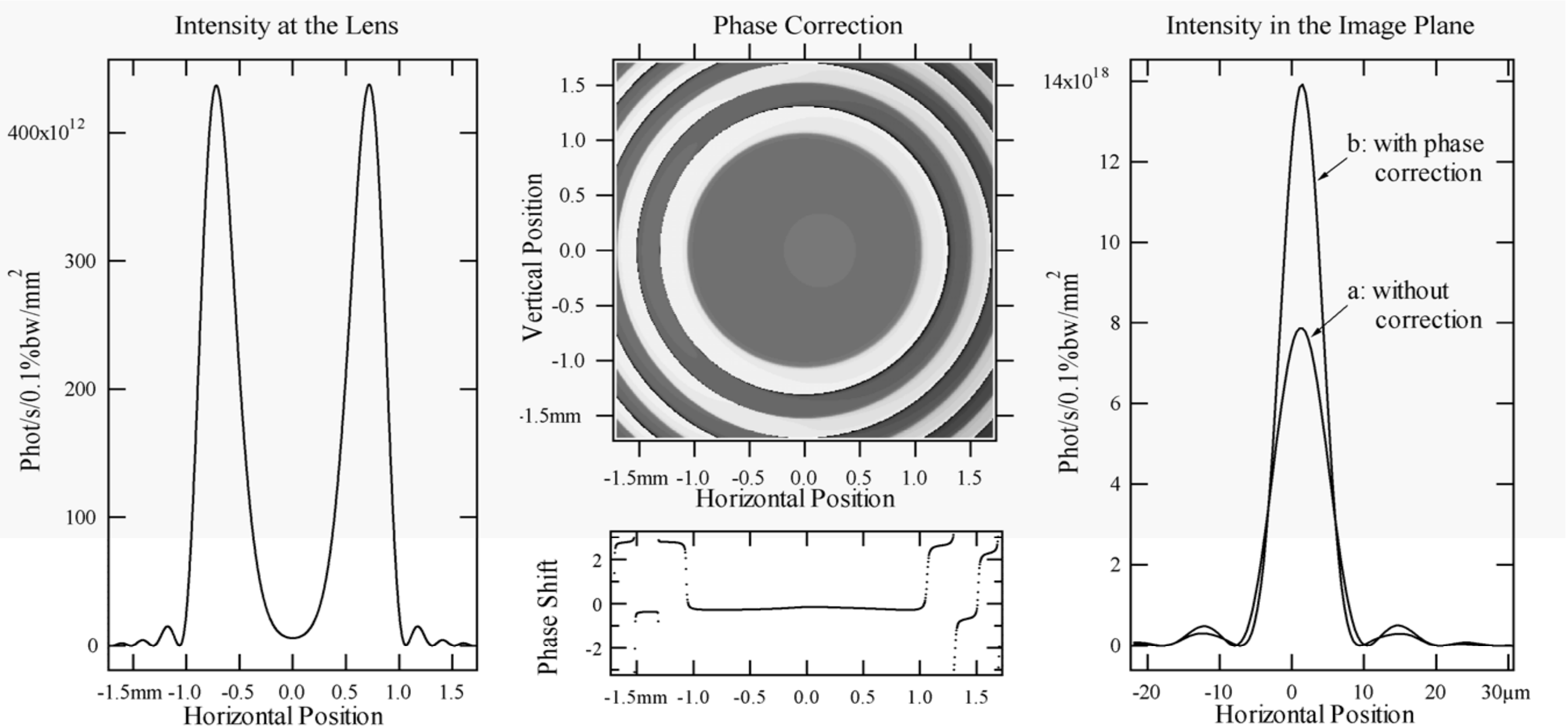

NIM-A, 1999

Examples: Wavefront Propagation

Peculiarities of UR Wavefronts

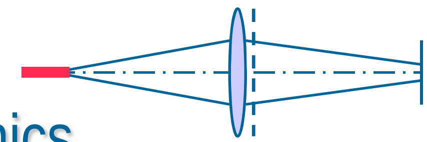

Planar Undulator, Even Harmonics

E = 6 GeV; K = 2.2; 38 x 42 mm; ε = 4.775 keV ($2^{\text{-nd}}$ harmonic)

1 : 1 imaging; 30 m from middle of Undulator to Thin Lens & Phase Correction

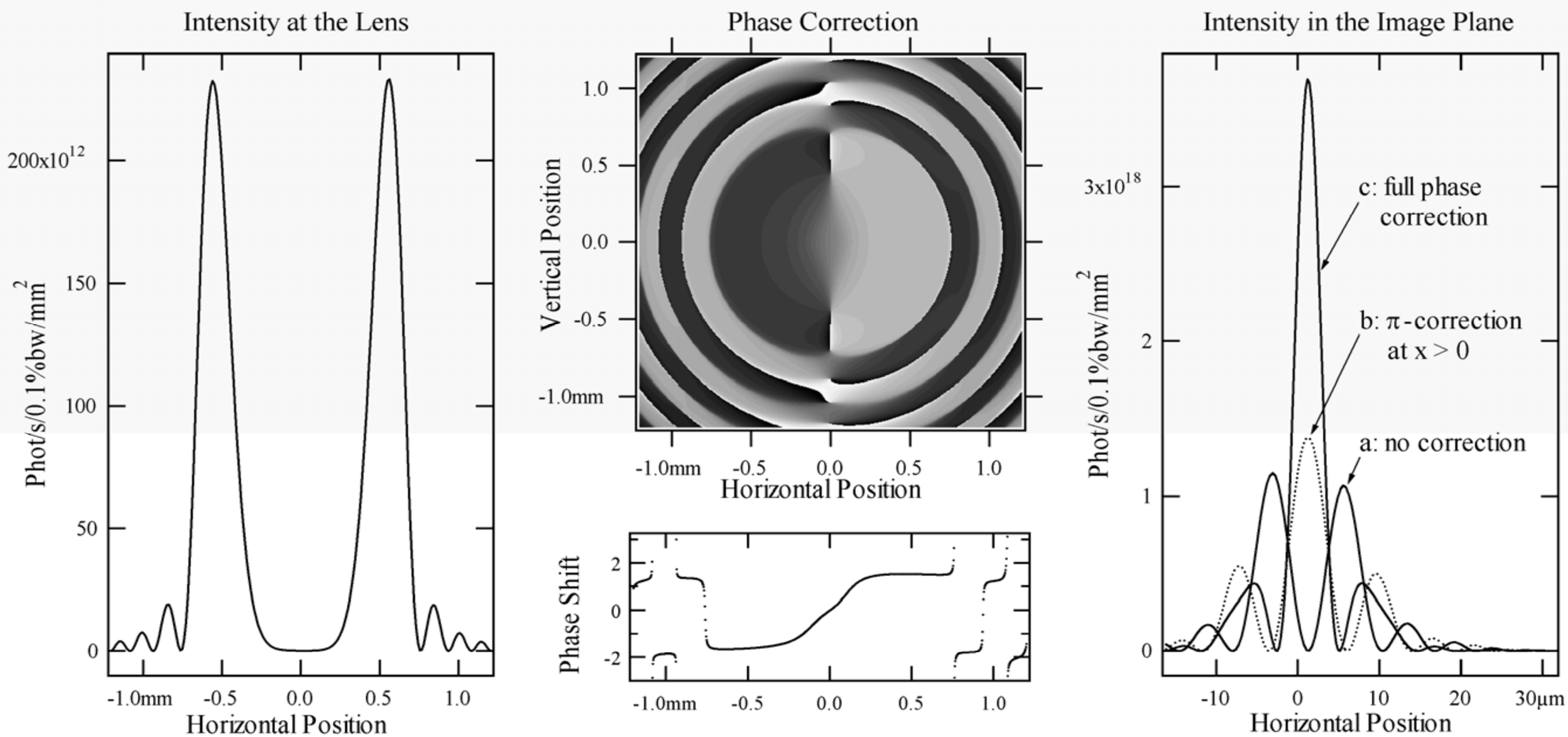

Examples: Wavefront Propagation

Peculiarities of UR Wavefronts

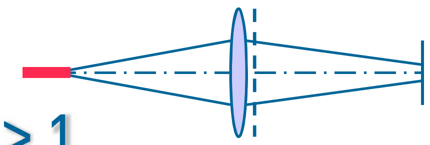

Helical Undulator, Harmonics n > 1

E = 6 GeV; $B_{x\,max} = B_{z\,max}$ = 0.3 T; 28 x 52 mm; ε = 4.20 keV (2^{-nd} harmonic)

1 : 1 imaging; 30 m from middle of Undulator to Thin Lens & Phase Correction

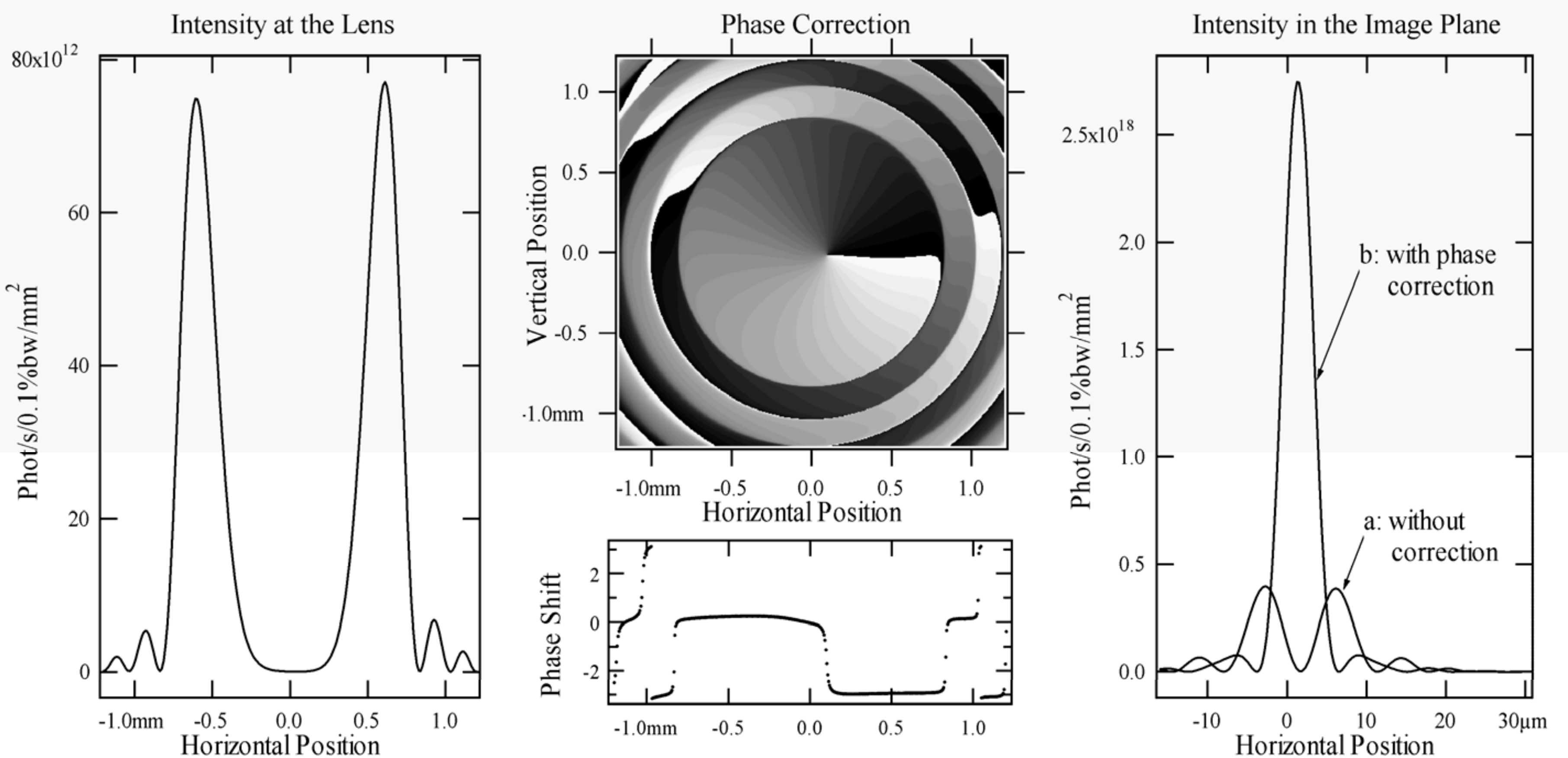

Directly relevant to “OAM”! – S. Sasaki and I. McNulty, PRL, 2008

Examples: Wavefront Propagation

Peculiarities of UR Wavefronts

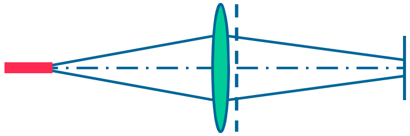

Focusing of Radiation from Helical Undulator, Harmonics n > 1

E = 6 GeV; $B_{x\,max} = B_{z\,max} = 0.3$ T; 28 x 52 mm; $\varepsilon = 4.20$ keV (2^{-nd} harmonic)

1 : 1 imaging; 30 m from middle of Undulator to Thin Lens & Phase Correction

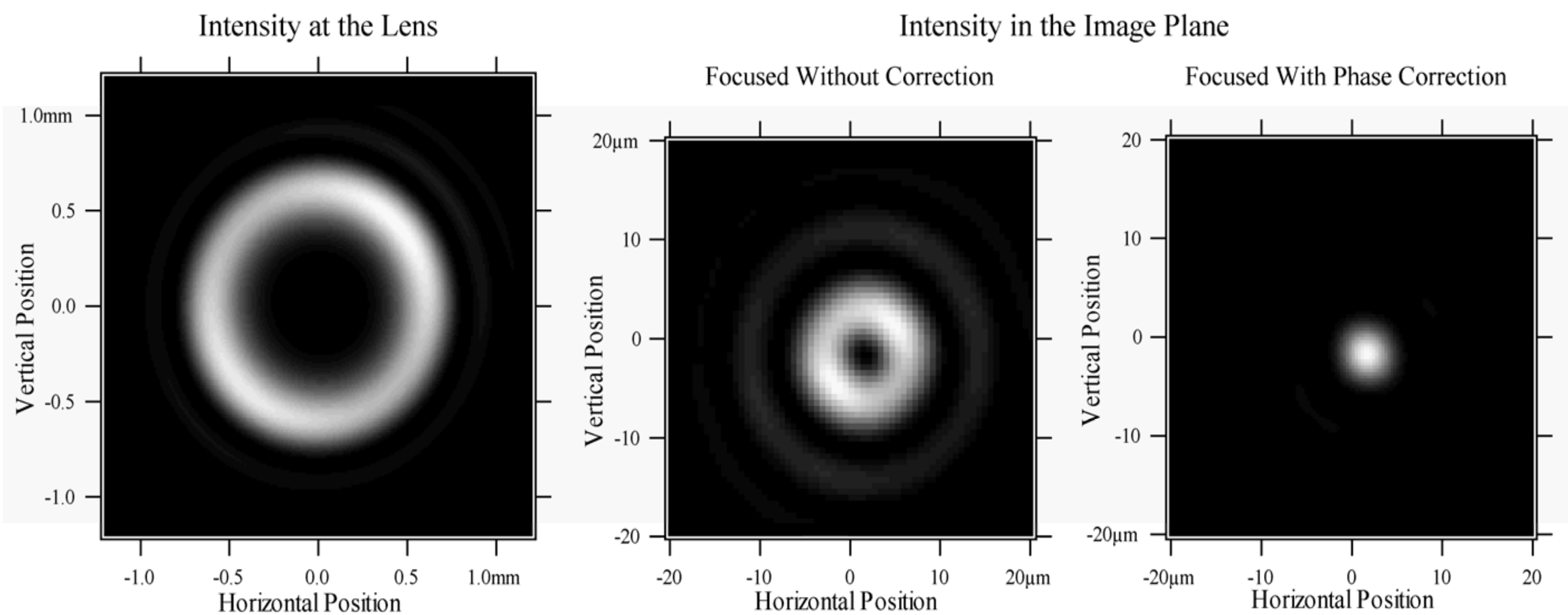

Wavefront Propagation Simulations for HU80-μFoc
Back-Propagation from M1 to Undulator Center (≈ 1:1 Imaging)

Electron Trajectories
from Measured Magnetic Field

Gap: 30 mm
Phase: -20 mm

In Vertical Plane

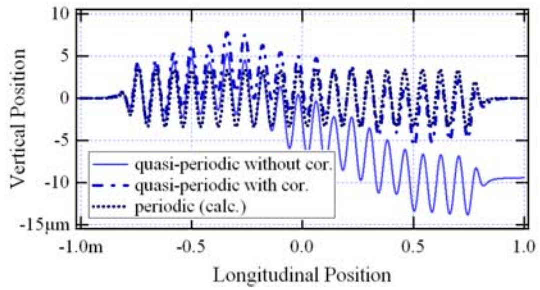

In Horizontal Plane

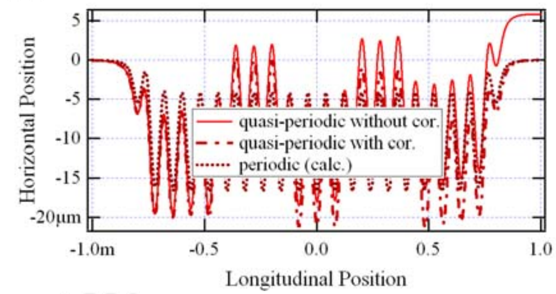

Intensity Distribution at M1
Photon Energy: 163 eV

Vertical Cuts

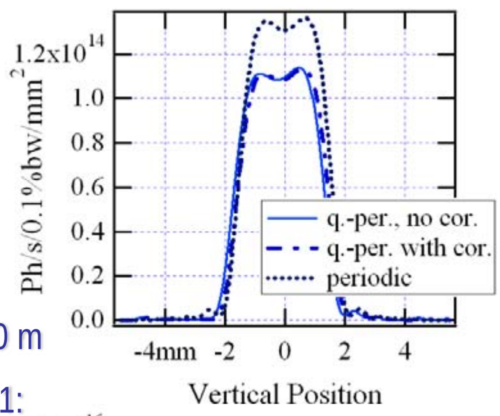

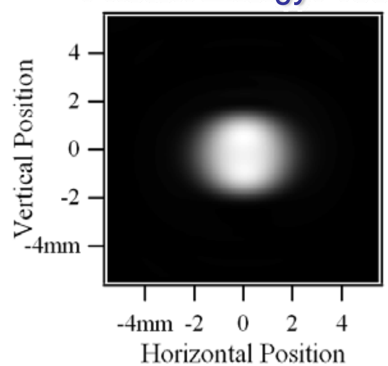

Horizontal Cuts

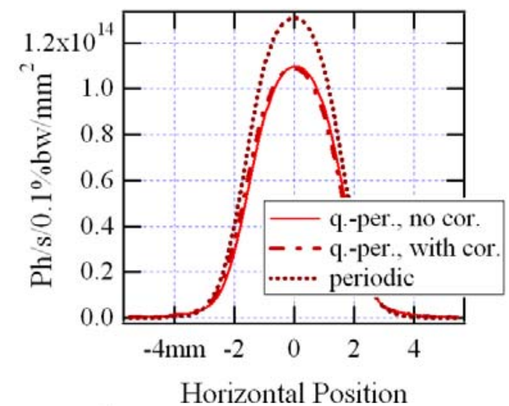

Distance from Und. to M1: 20 m

Aperture @ M1:
5 mm (H) x
4 mm (V)

Intensity Distribution after Back-Propagation

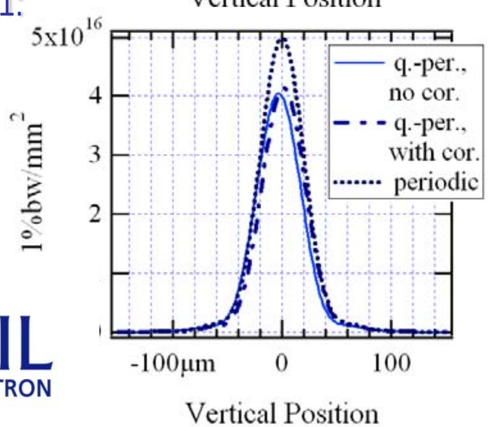

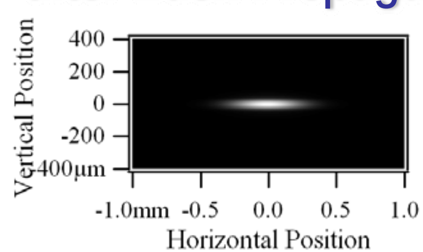

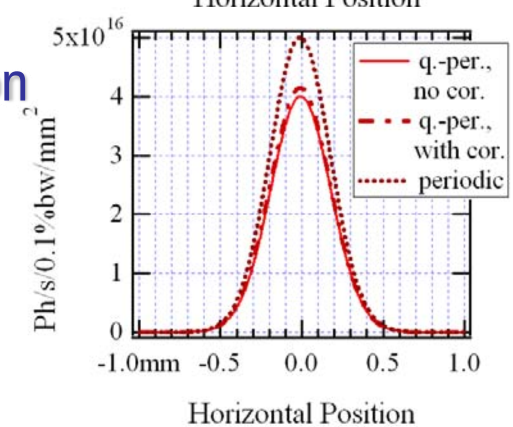

SOLEIL SYNCHROTRON

Partially-Coherent Wavefront Propagation Simulations for Phase-Contrast Tomography BL: Approximate Scheme

Optical Scheme

A. Somogyi, T. Moreno, F. Polack

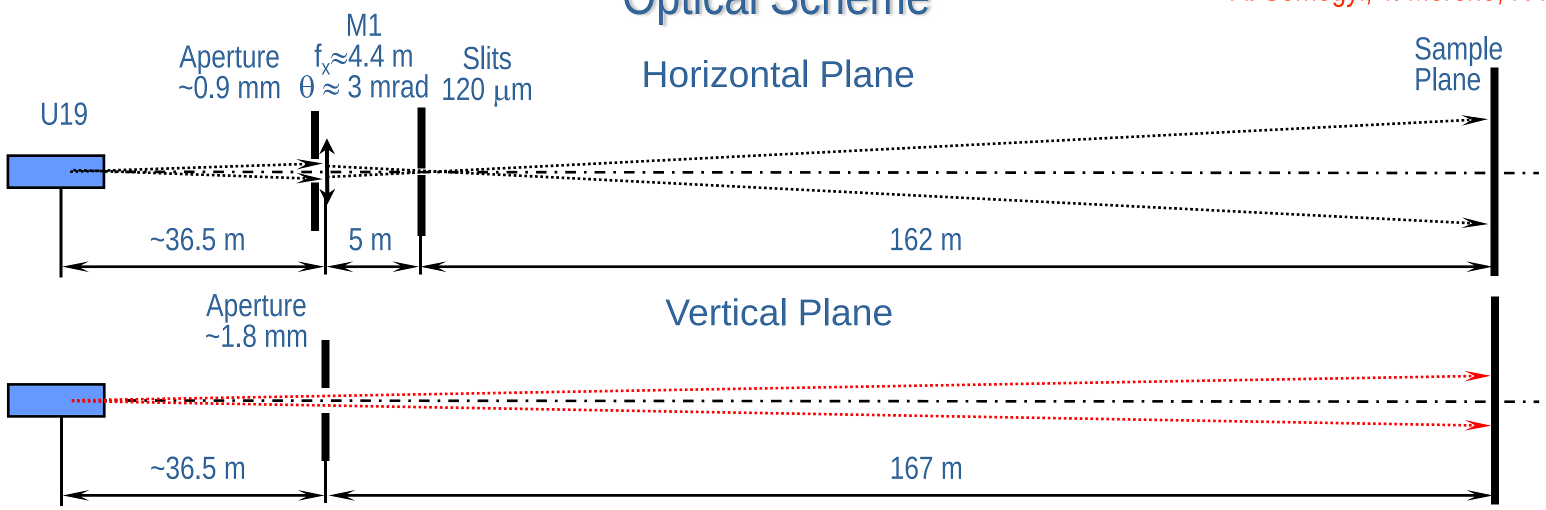

Intensity Distributions in Transverse Plane at Sample (no Slope Error, ε ≈ 10 keV)

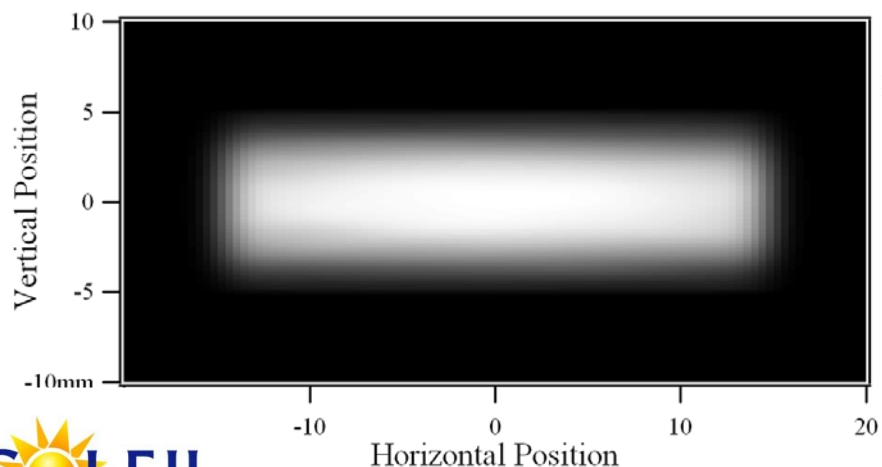

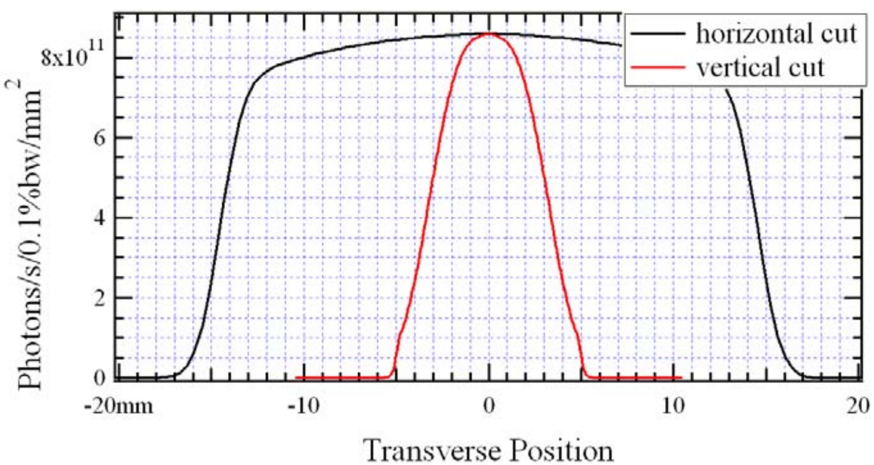

Partially-Coherent Wavefront Propagation Simulations for Tomography BL: M1 Slope Error Effect

Modeling Surface Height Profile (due to Slope Error) of Horizontally-Focusing Mirror

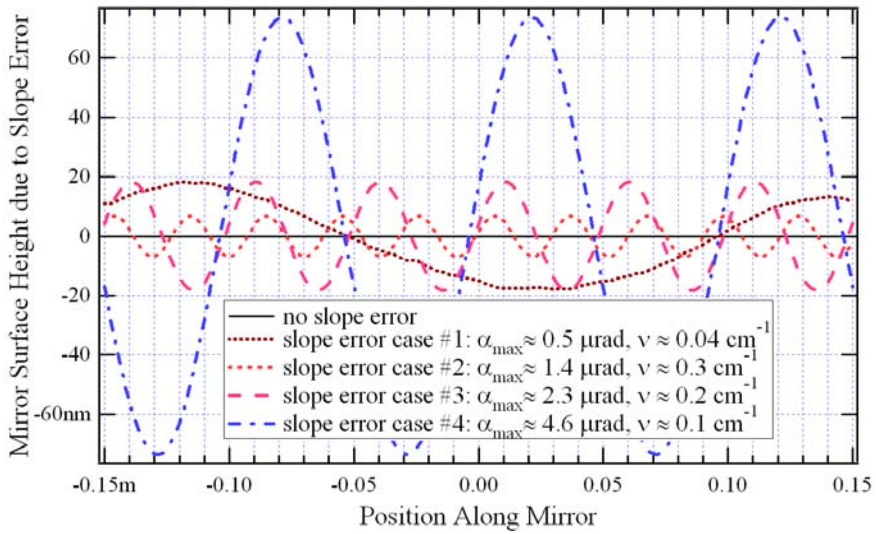

Horizontal Cuts of Intensity Distributions at Sample

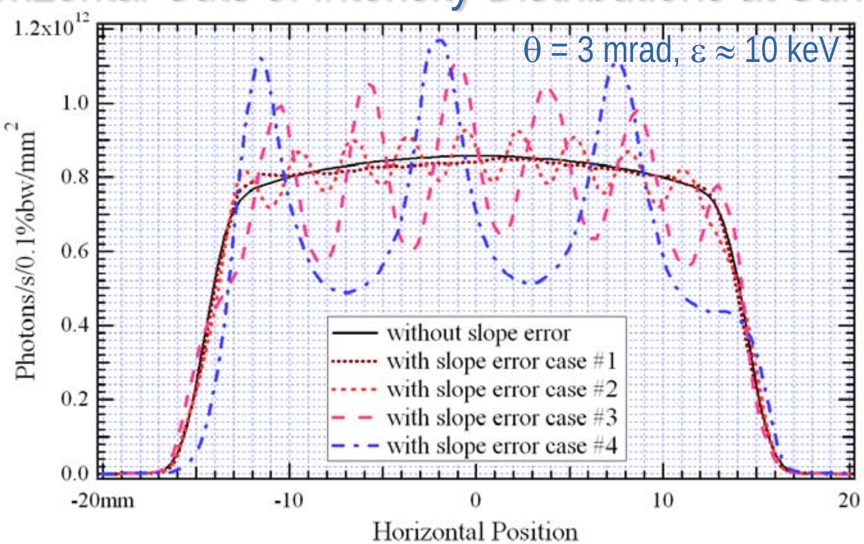

Intensity Distributions at Sample

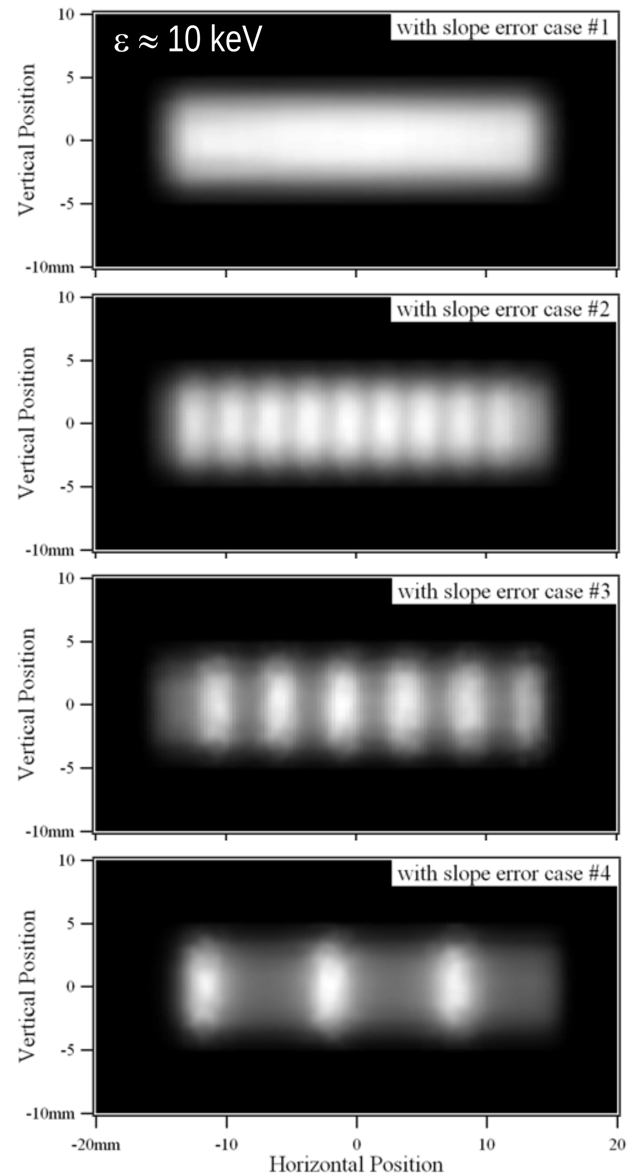

M1 Slope Error Effects for Different E-Beam Parameters

Modeling Surface Height Profile (due to Slope Error)

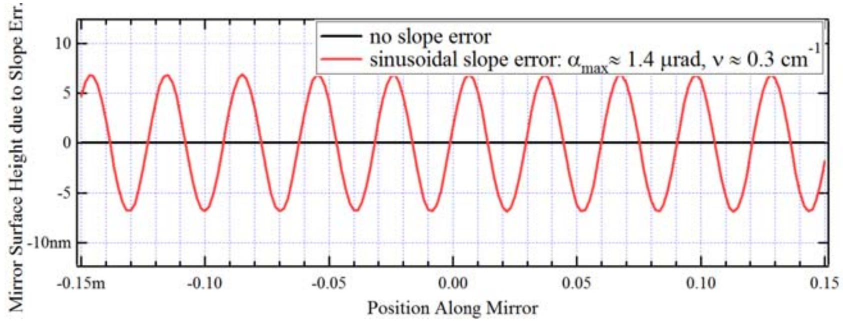

Intensity Distributions at Sample

θ = 3 mrad, $\varepsilon \approx$ 10 keV

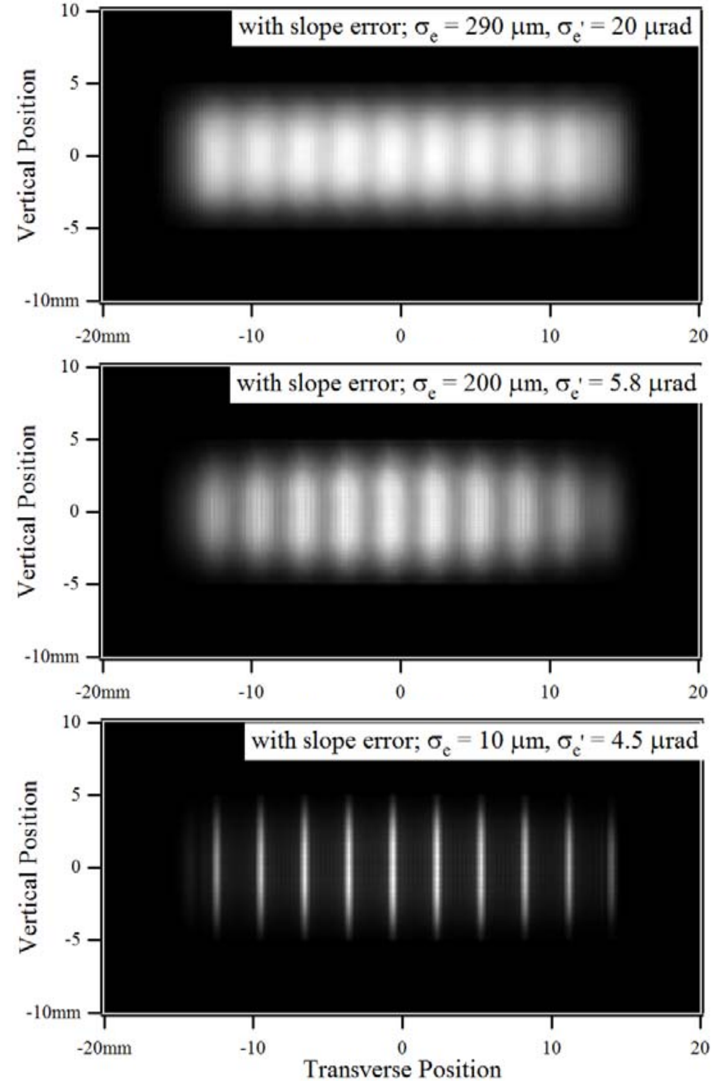

Cuts of Intensity Distributions at Sample

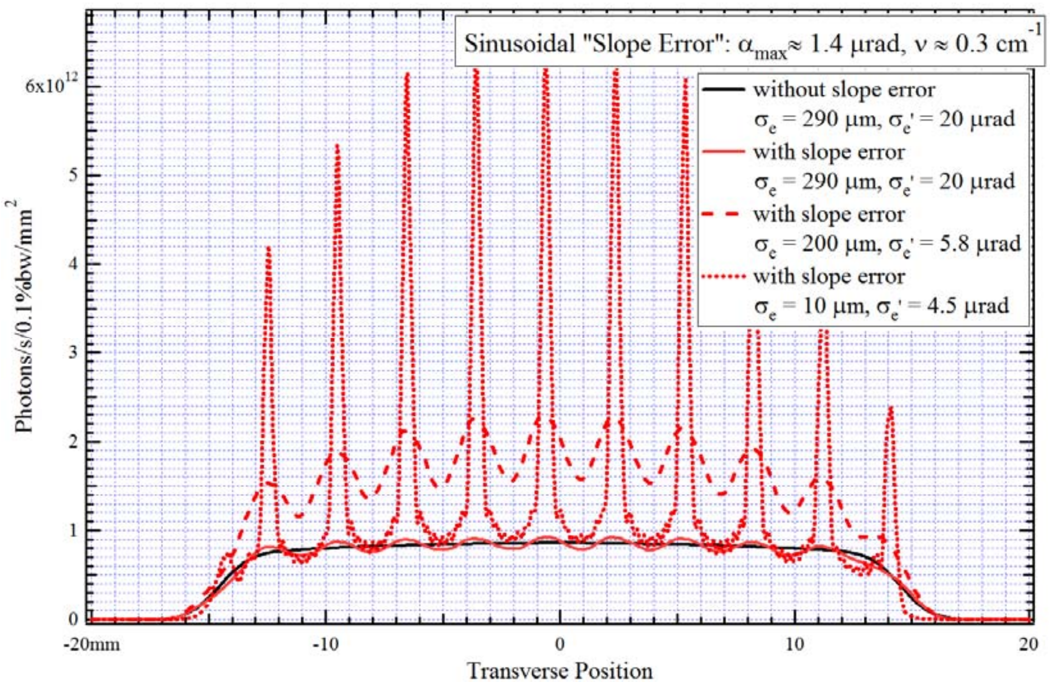

Partially-Coherent Wavefront Propagation Simulations for Phase-Contrast Tomography BL: Image of Sample Sphere

Optical Scheme

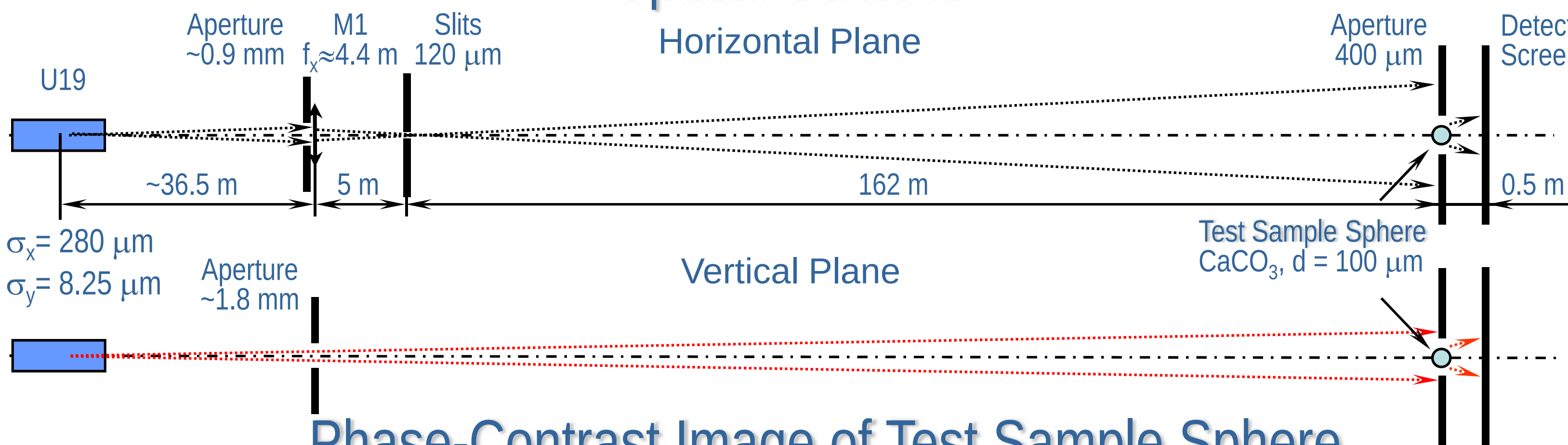

Phase-Contrast Image of Test Sample Sphere

Intensity Distribution at Detector Screen at $\varepsilon \approx 10$ keV, M1 Slope Error

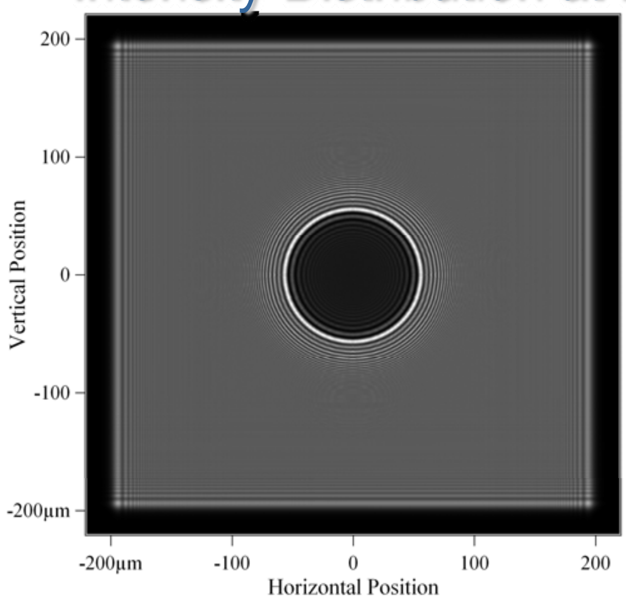

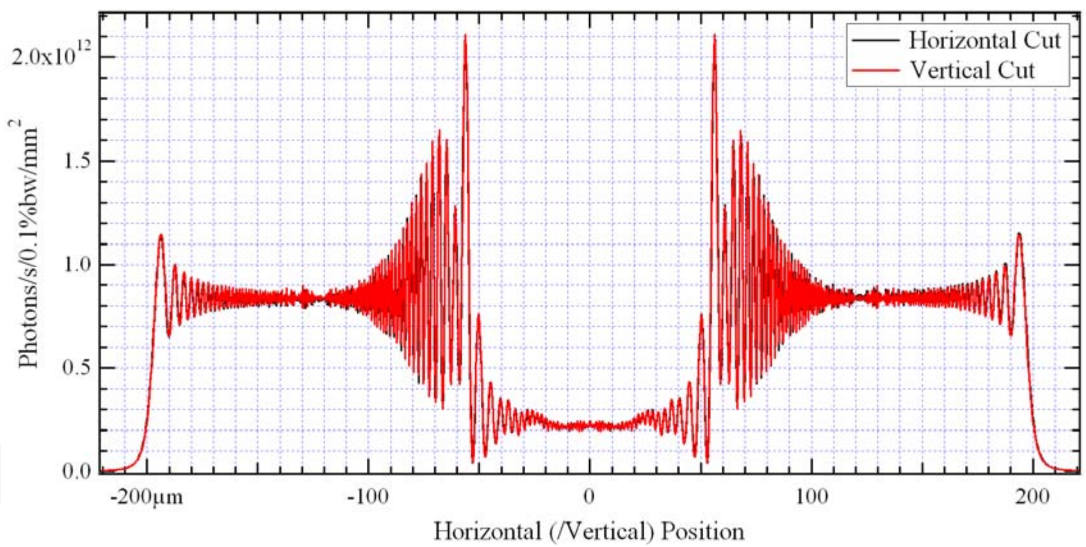

Preliminary Wavefront Propagation Calculations for MICROSCOPIUM: Standard Long Straight Section (A)

Lattice Functions

(Long Straight Section)

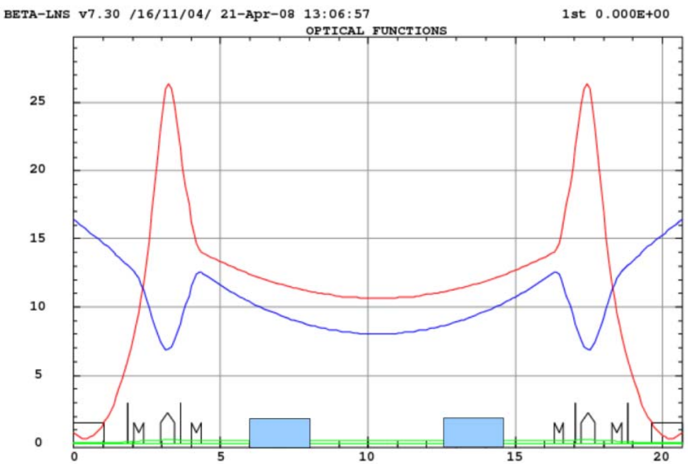

Intensity @ Sample

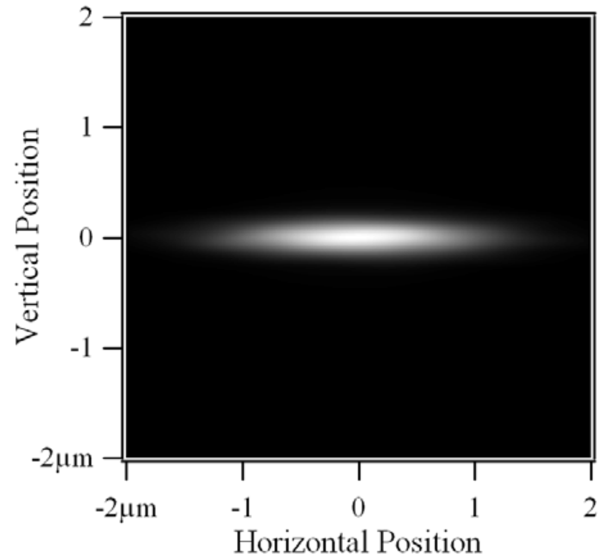

$\varepsilon \approx 10$ keV

Flux $\approx 5.2\times10^{12}$ Ph/s/0.1%bw

Optical Scheme (A)

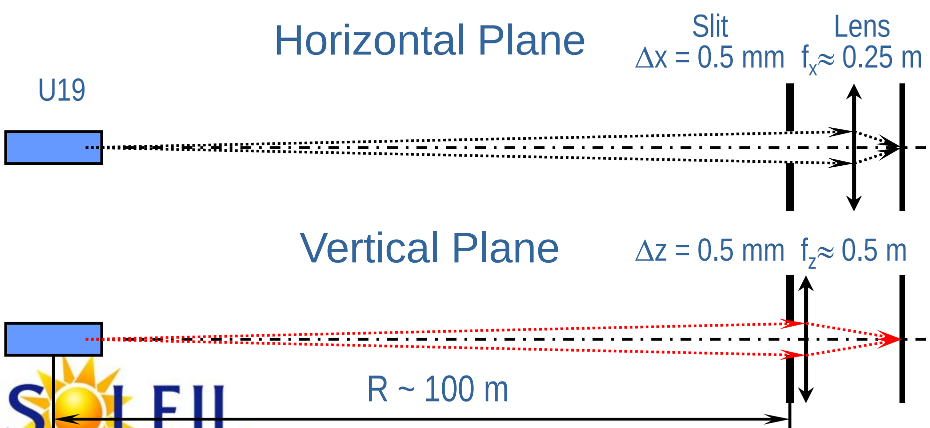

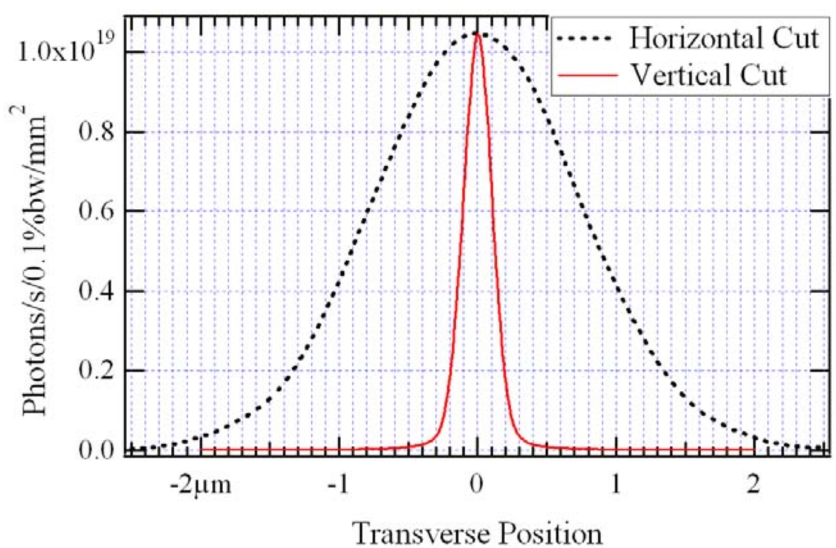

SOLEIL SYNCHROTRON

Preliminary Wavefront Propagation Calculations for MICROSCOPIUM: Standard Long Straight Section (B)

Lattice Functions
(Long Straight Section)

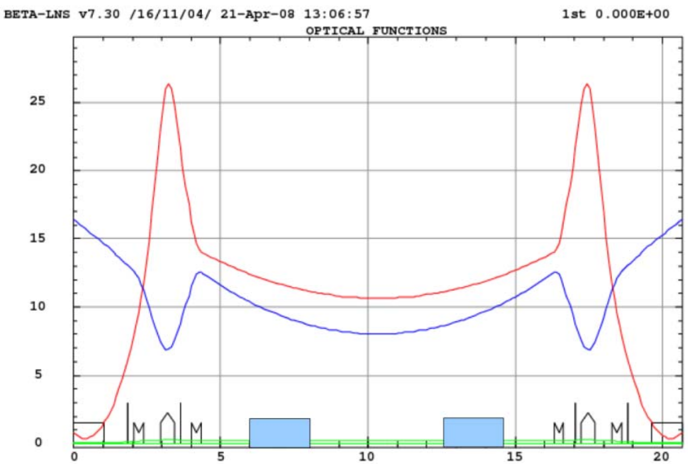

Intensity @ Sample

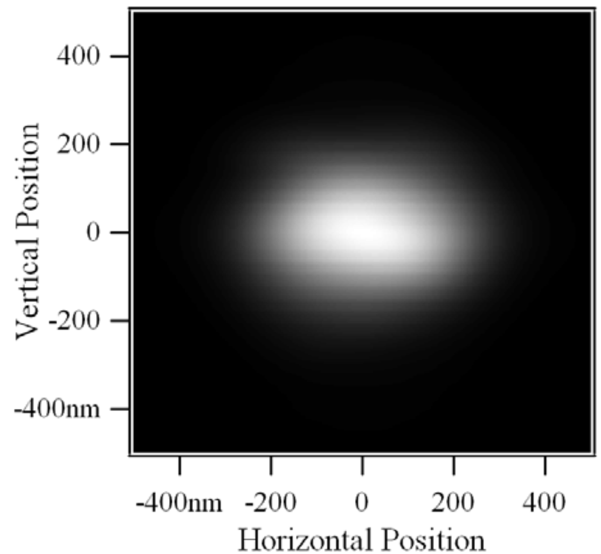

$\varepsilon \approx 10$ keV

Flux $\approx 1\times10^{12}$ Ph/s/0.1%bw

Optical Scheme (B)

Horizontal Plane

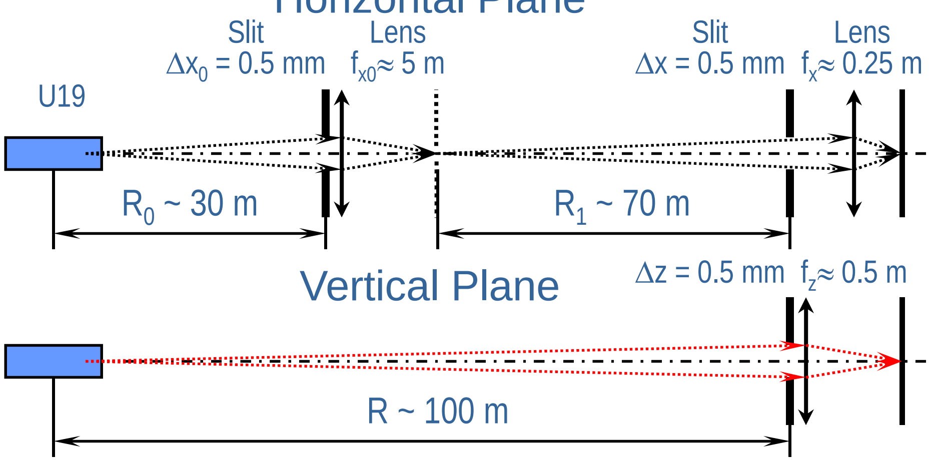

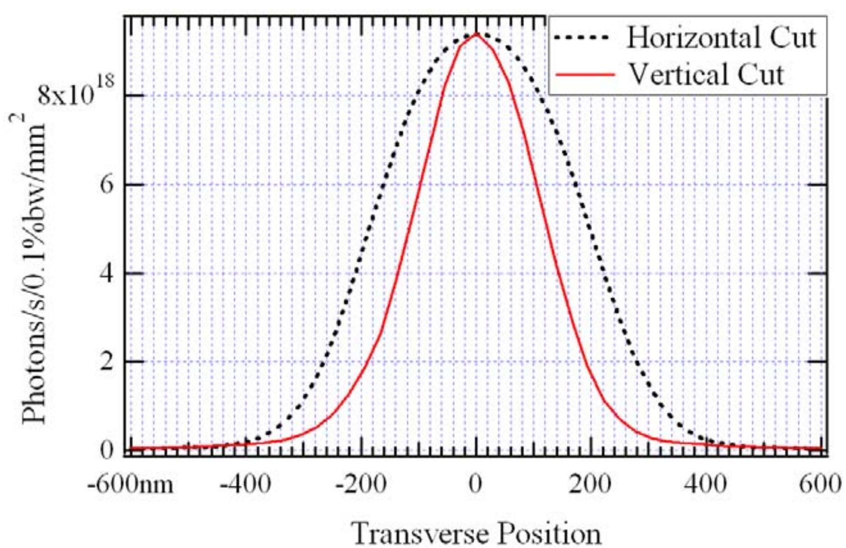

Preliminary Wavefront Propagation Calculations for MICROSCOPIUM: Modified Long Straight Section

Lattice Functions

(Modified Long Straight Section)

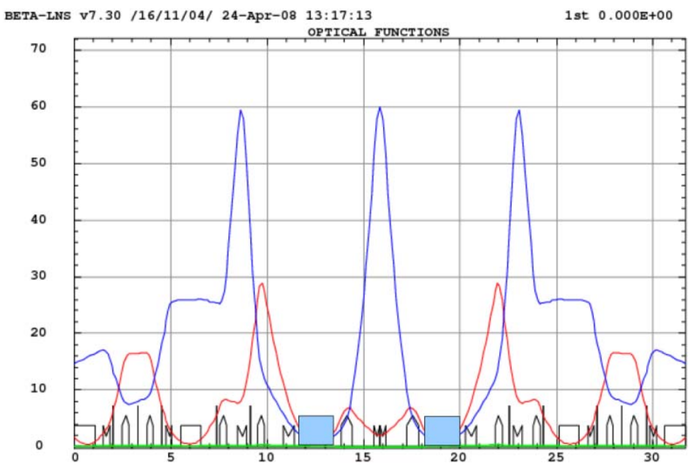

Intensity @ Sample

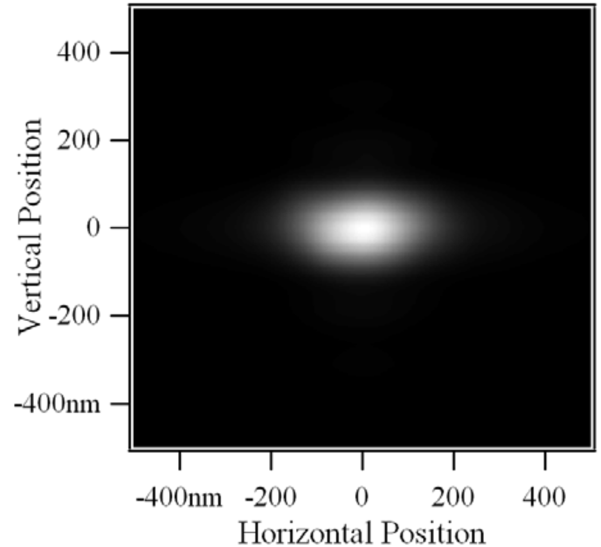

$\varepsilon \approx 10$ keV

Flux $\approx 7.5\times10^{11}$ Ph/s/0.1%bw

Optical Scheme (A)

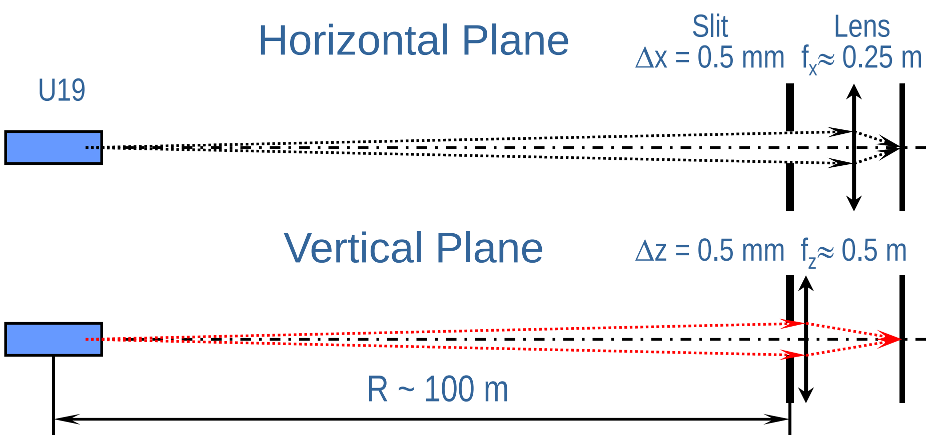

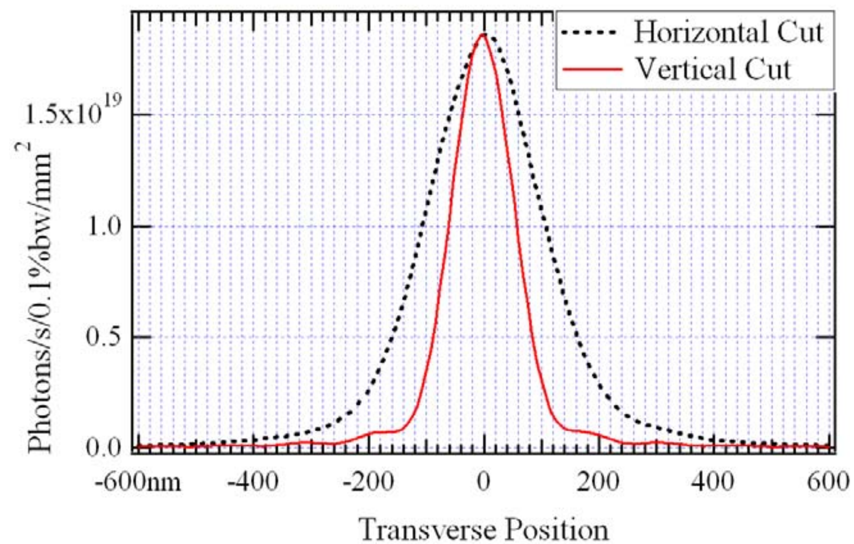

Wavefront Propagation Calculations for MICROSCOPIUM: Comparison of Optical Schemes with Zone Plates

Optical Schemes

(I)

Horizontal Plane

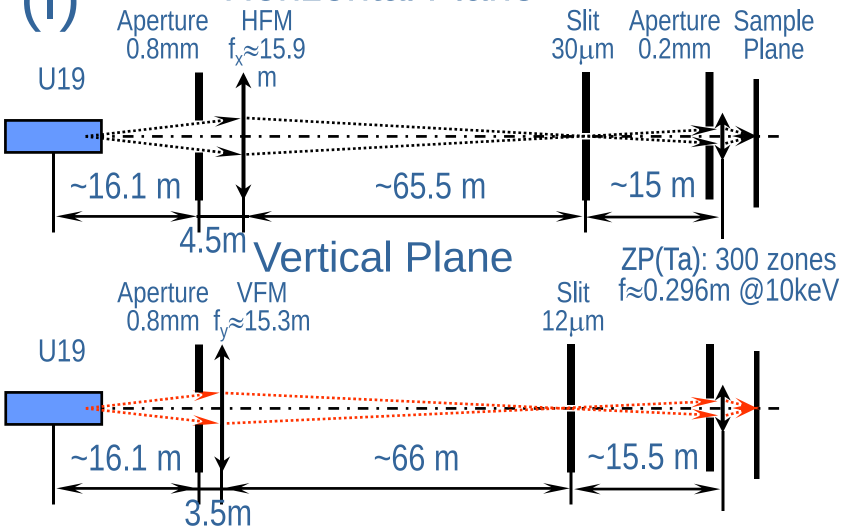

Intensity and Flux at Sample

Photon Energy: 10 keV

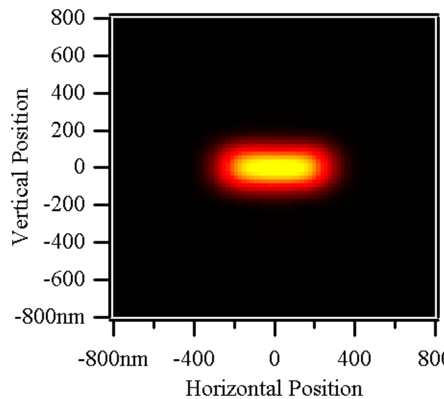

ZP Efficiency ~ 0.11

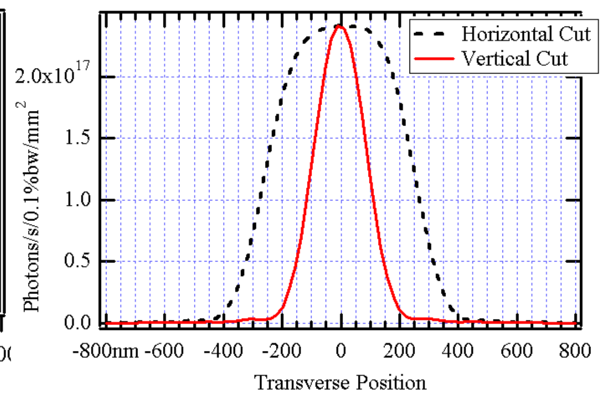

Flux ≈ 2.9×10^{10} Ph/s/0.1%bw

(II)

Horizontal Plane

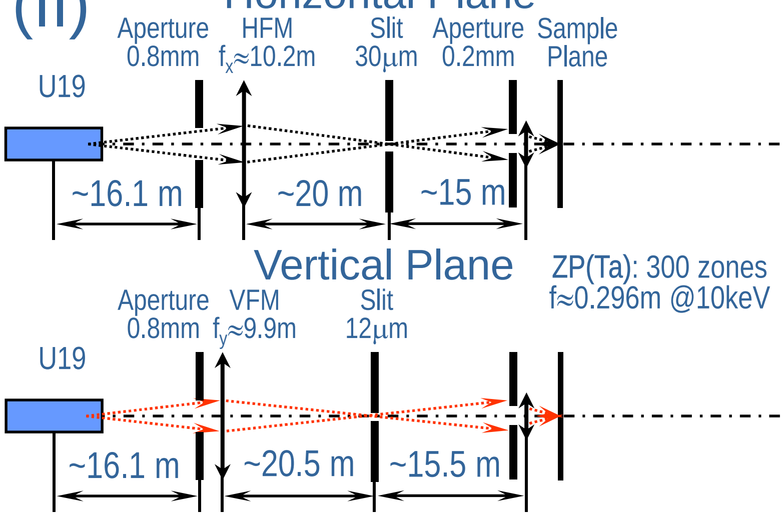

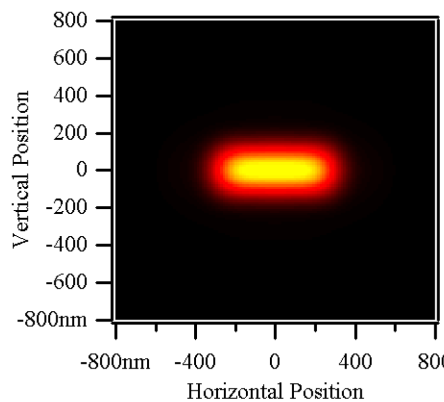

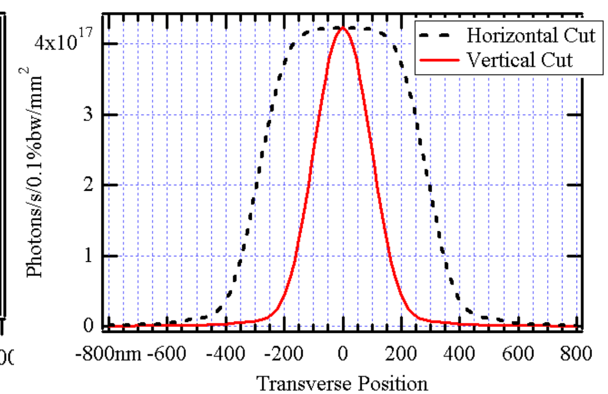

Flux ≈ 6.6×10^{10} Ph/s/0.1%bw

A. Somogyi, T. Moreno, F. Polack

Examples: Wavefront Propagation

X-Ray Focusing Using a Zone Plate (Full Transverse Coherence)

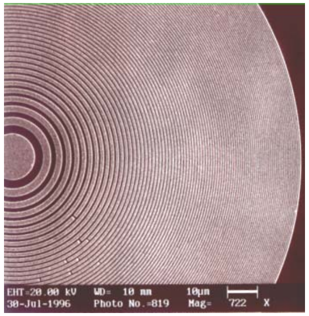

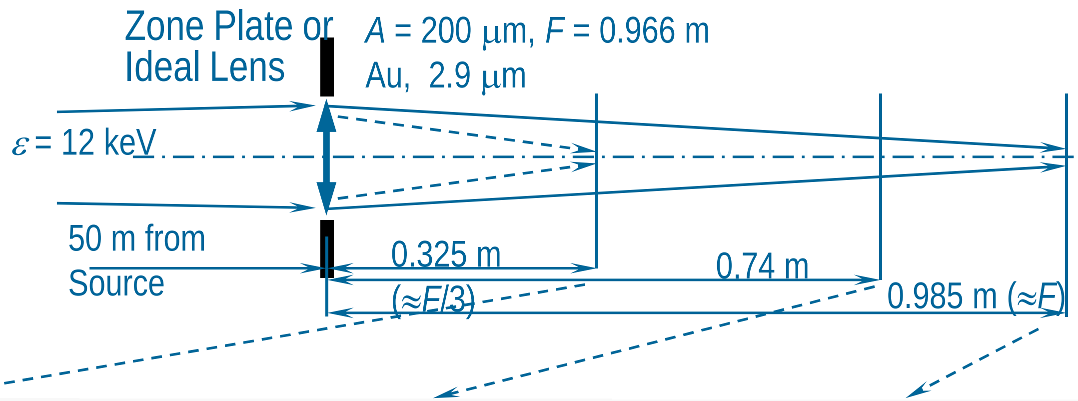

Zone Plate

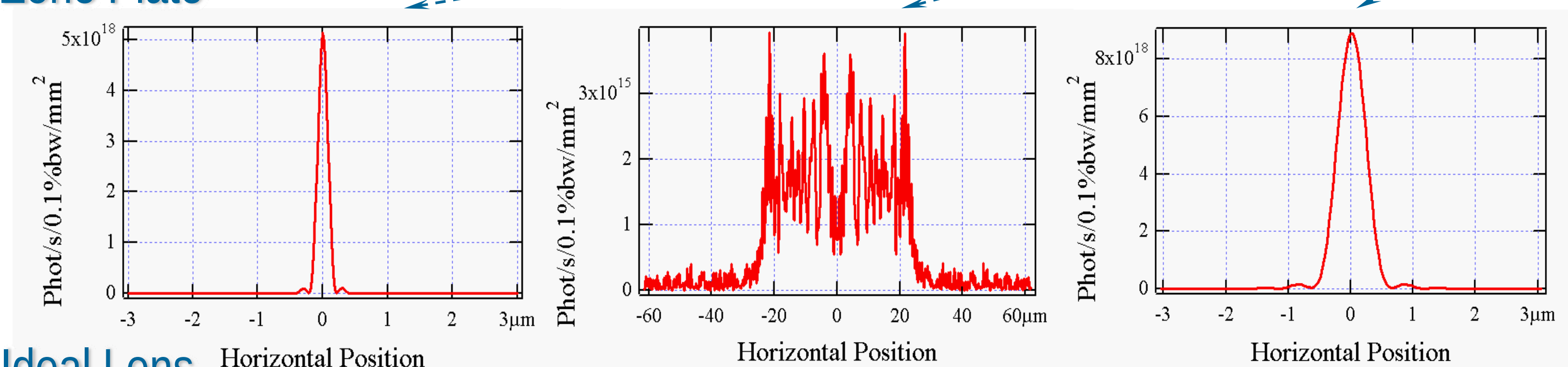

Ideal Lens

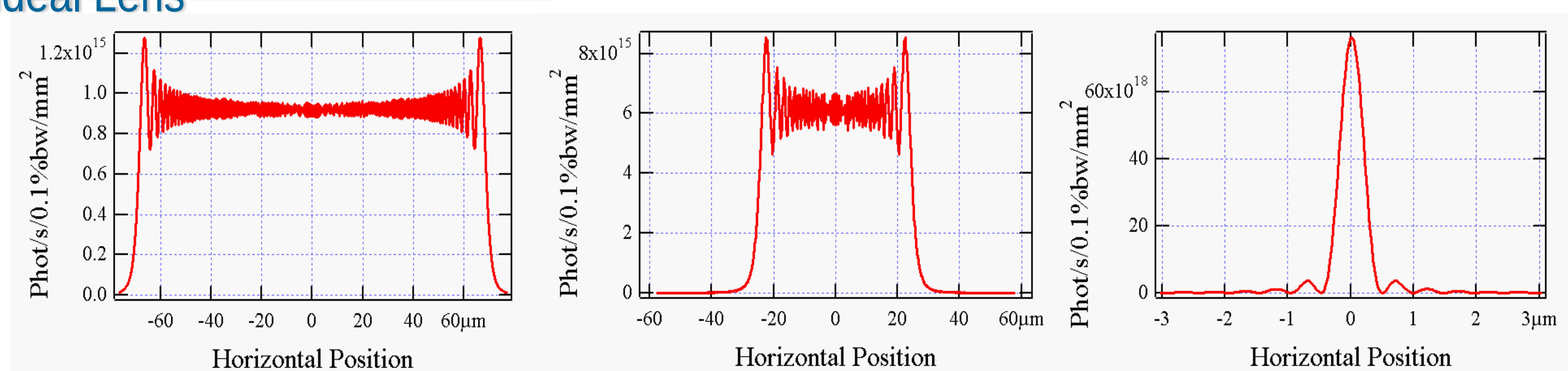

Examples: Wavefront Propagation

X-Ray Focusing Using a Zone Plate (Partial Coherence)

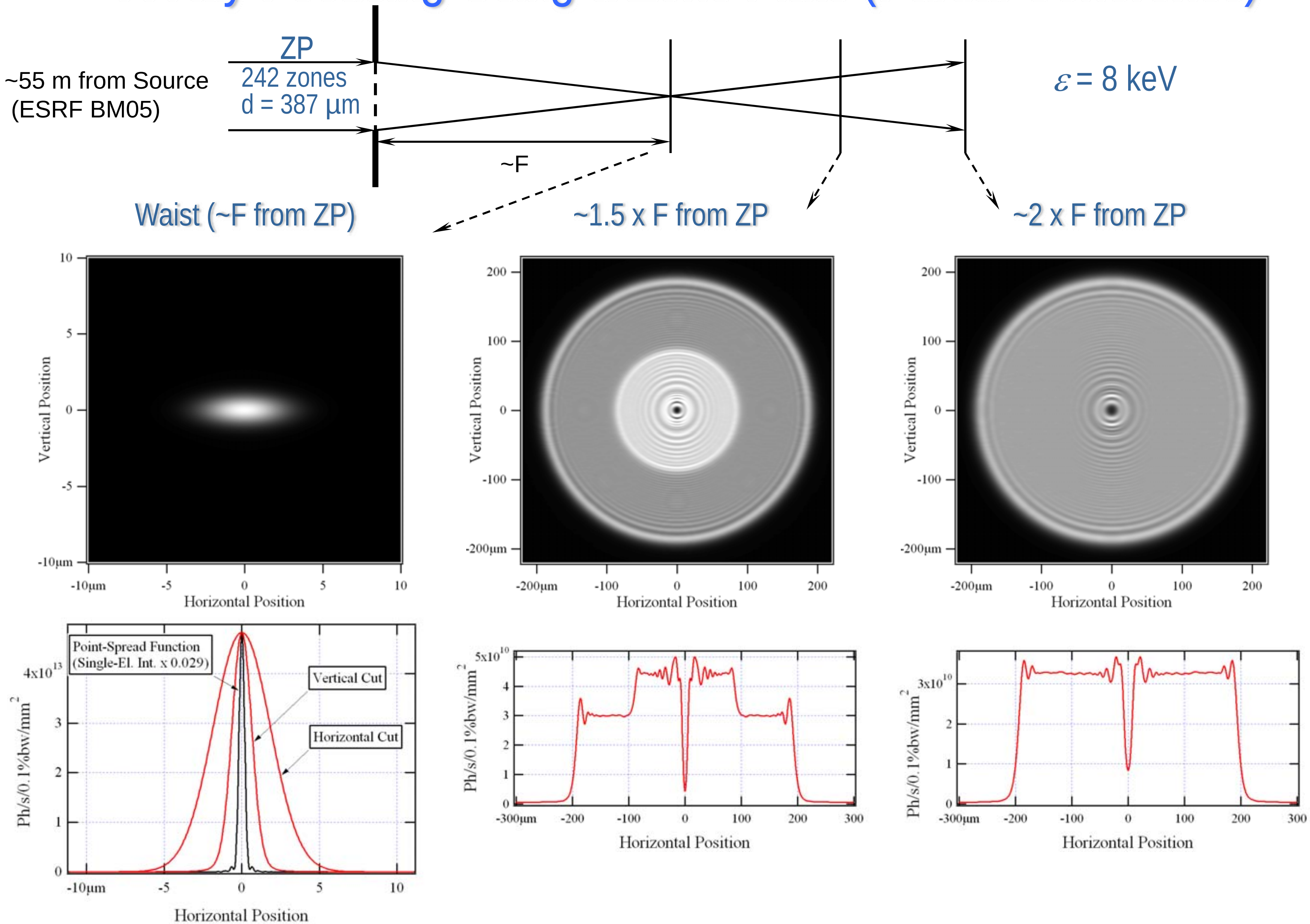

Examples: Wavefront Propagation / Analysis

Partially Coherent X-Rays Observed Out of Focus of a Zone Plate

Aperture at Waist:
600 μm x 600 μm

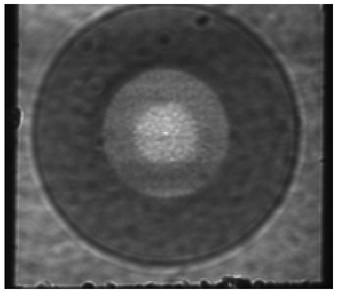

Intensity Distributions
at 0.55 m after Waist

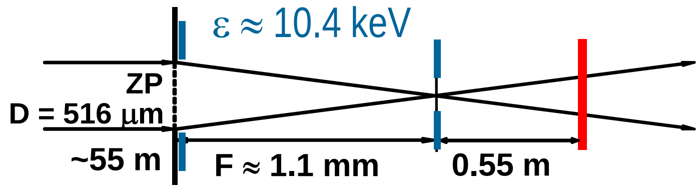

Aperture at Waist:
10 μm x 10 μm

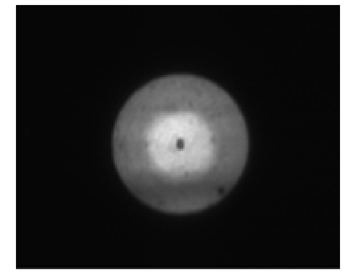

Measurements (ESRF BM5)
M.Idir, A.Snigirev et. al.

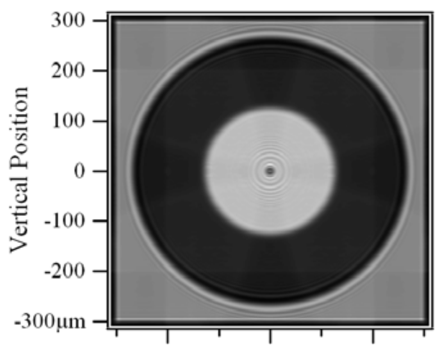

Calculation for Perfect ZP

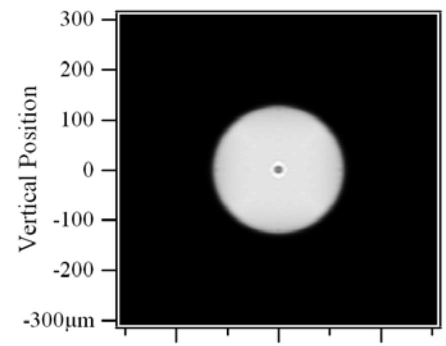

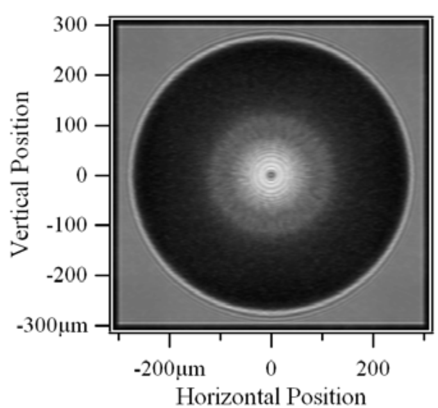

Calculation for ZP
with non-perfect outer zones

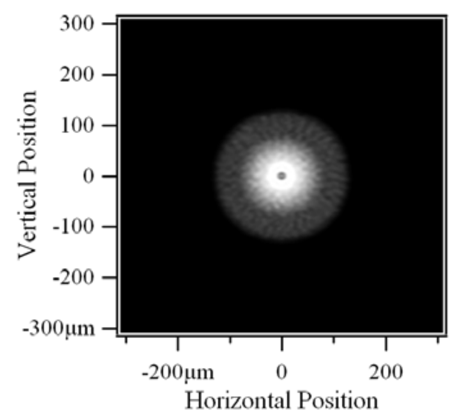

Examples: Wavefront Propagation

Point-Spread Function Computation for Parabolic X-Ray CRL

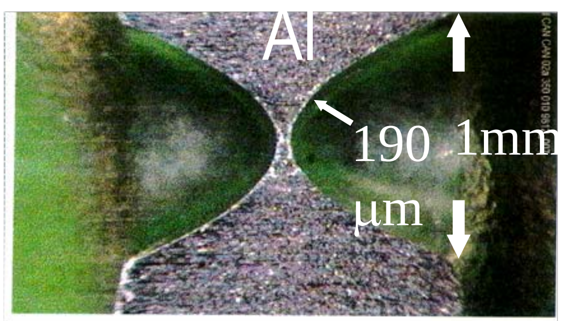

A.Snigirev, B.Lengeler, et. al., 1998

ε = 8.9 keV

$\delta = 6.9 \times 10^{6}$

L_{atten} = 0.106 mm

N = 1

F = 13.6 m

Δ_{FWHM} = 7.3 μm

ε = 23 keV

$\delta = 1. \times 10^{6}$

L_{atten} = 1.89 mm

N = 7

F = 13.1 m

Δ_{FWHM} = 4.1 μm

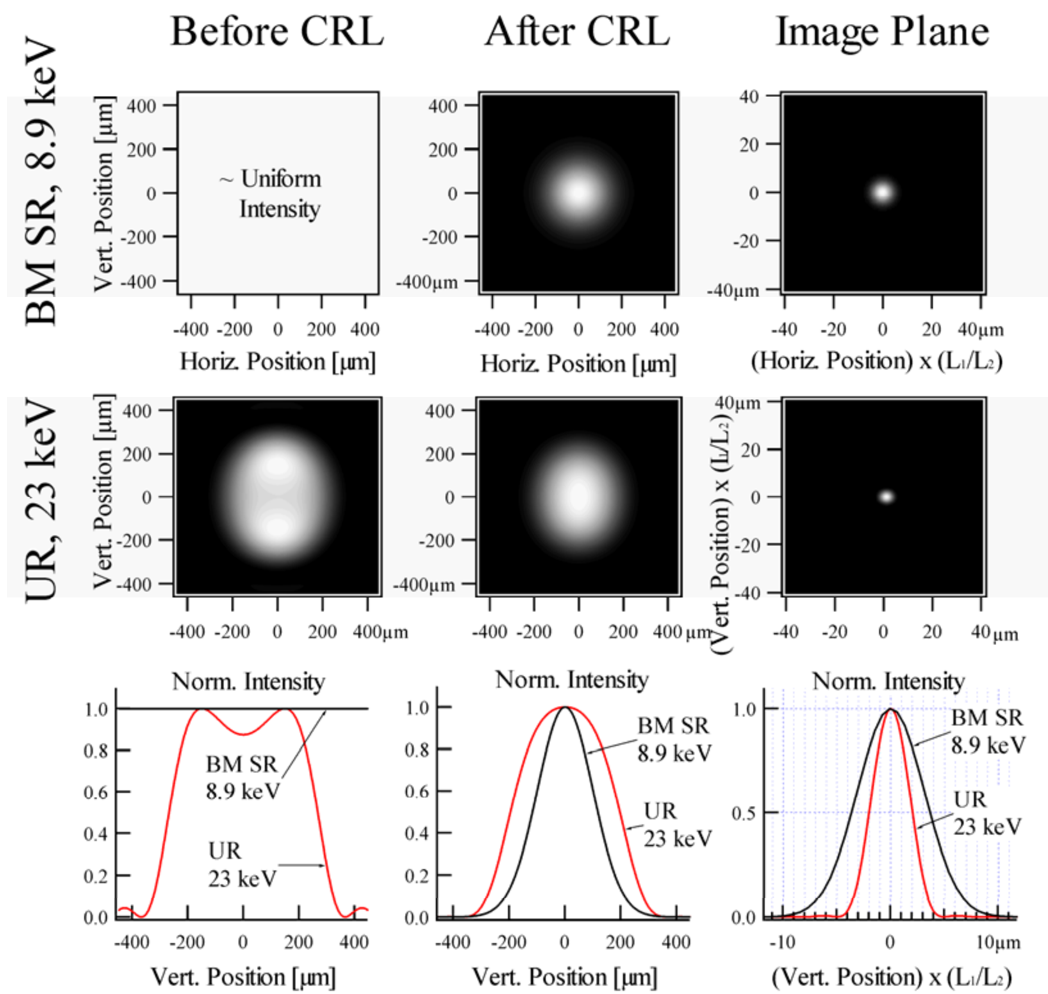

Examples: Wavefront Propagation

Fresnel Diffraction of Partially Coherent X-Rays

Measurements by A.Snigirev et. al.

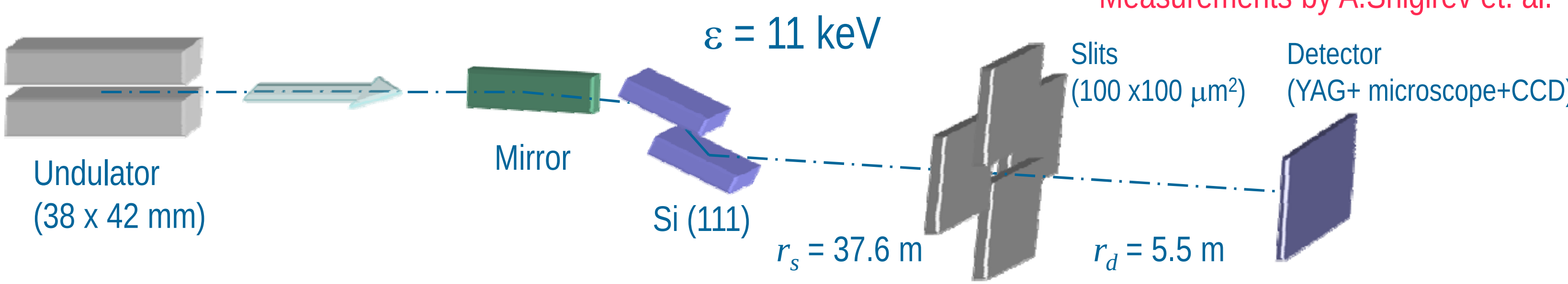

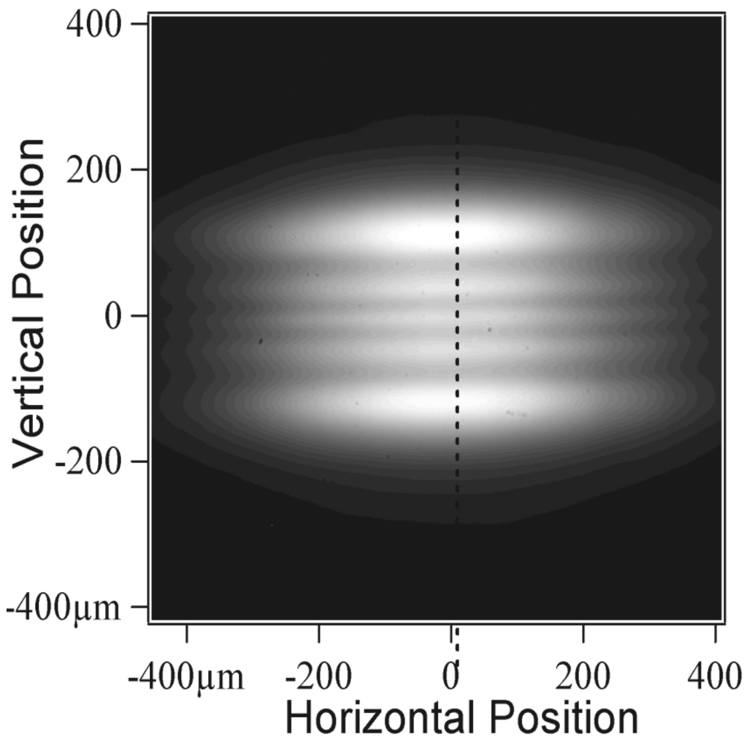

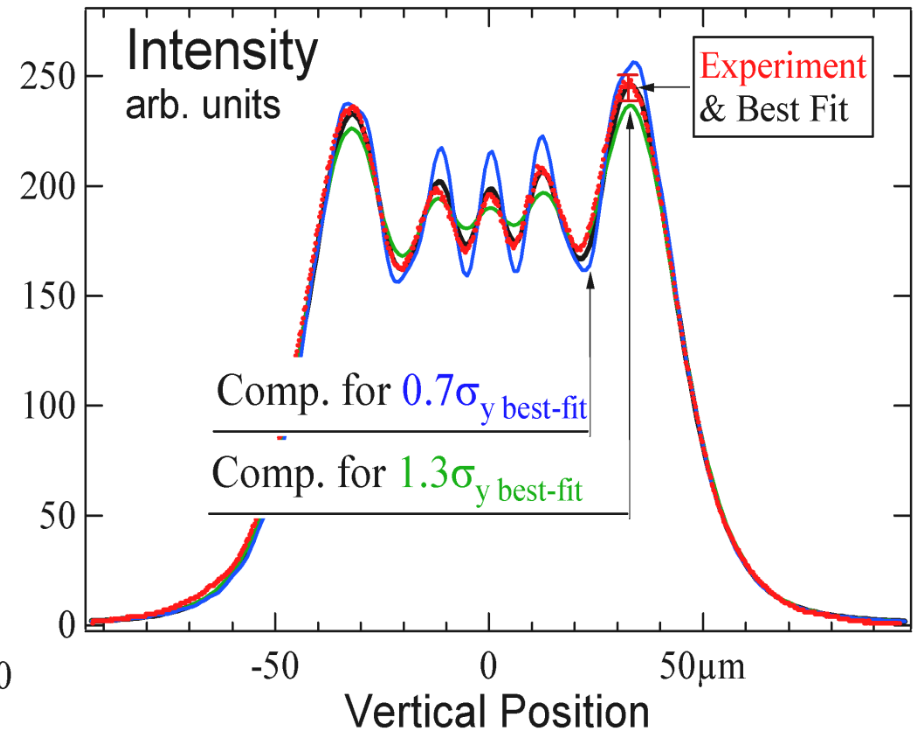

Examples: Wavefront Propagation

Interference of Partially Coherent X-Rays

A.Snigirev et. al.

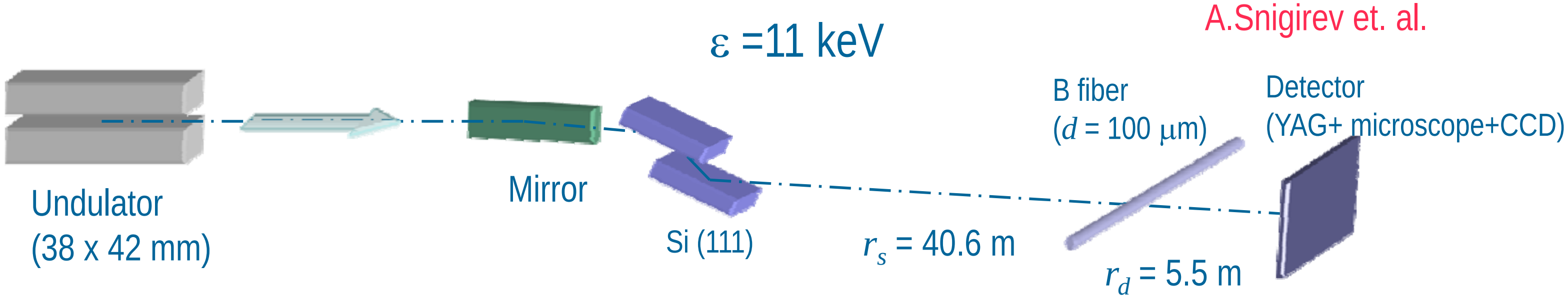

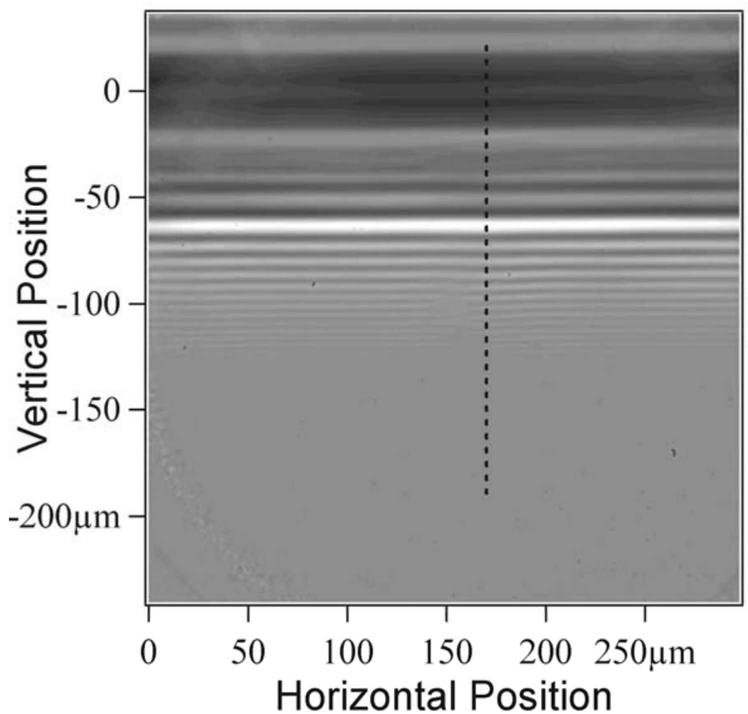

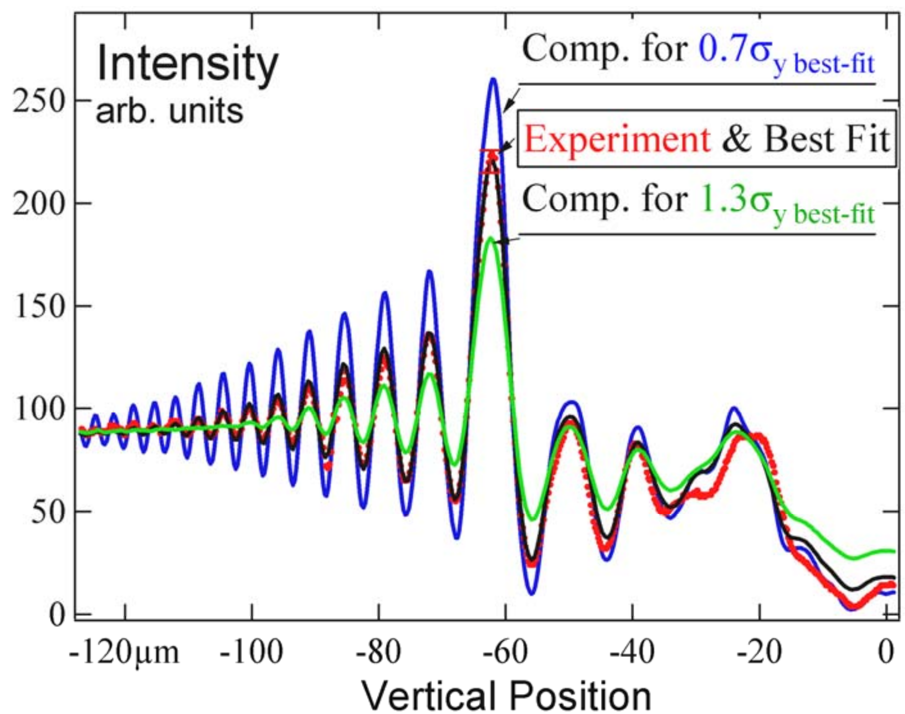

Resolution of the Well-Known X-ray Pinhole Camera

ESRF Pinhole Camera by P. Elleaume et. al. (1995)

SOLEIL version by M.-A. Tordeux et. al. (DIPAC-2007)

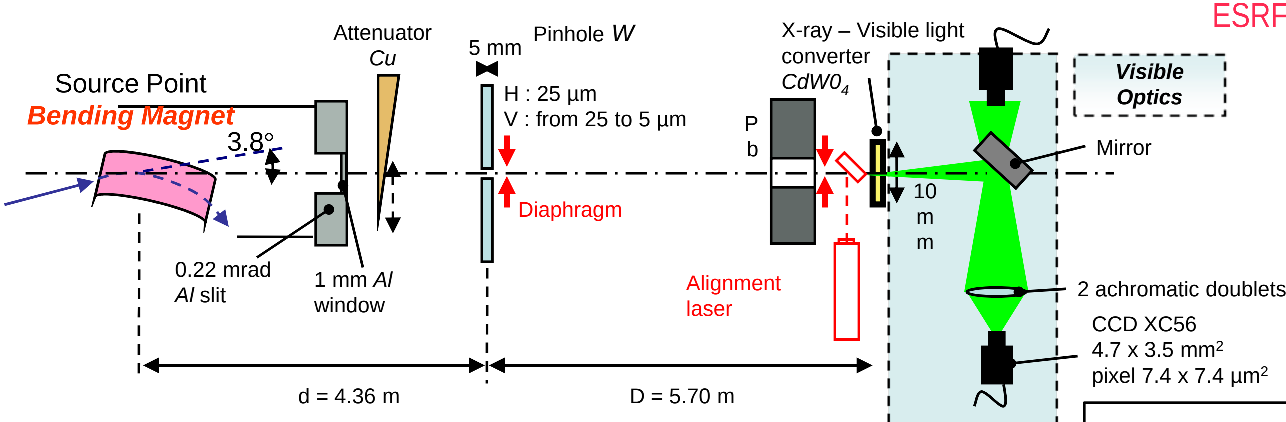

Resolution
vs Pinhole Size
for Diff. Attenuator Thickness

Quadratic sum of the Geometry and Fraunhofer Diffraction contributions

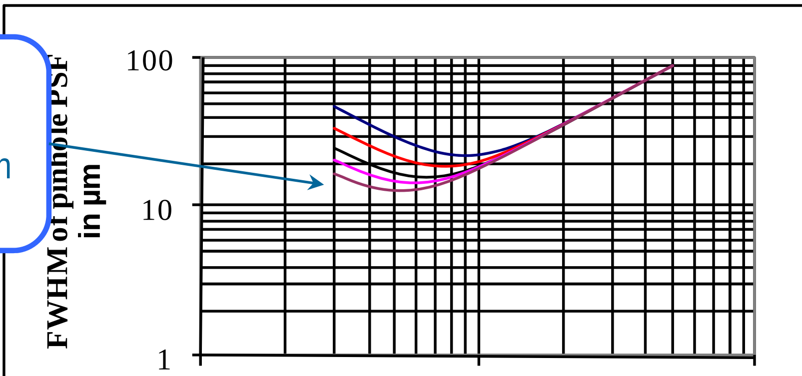

Wave-optics calculation (Fresnel Diffraction of Polychromatic SR)

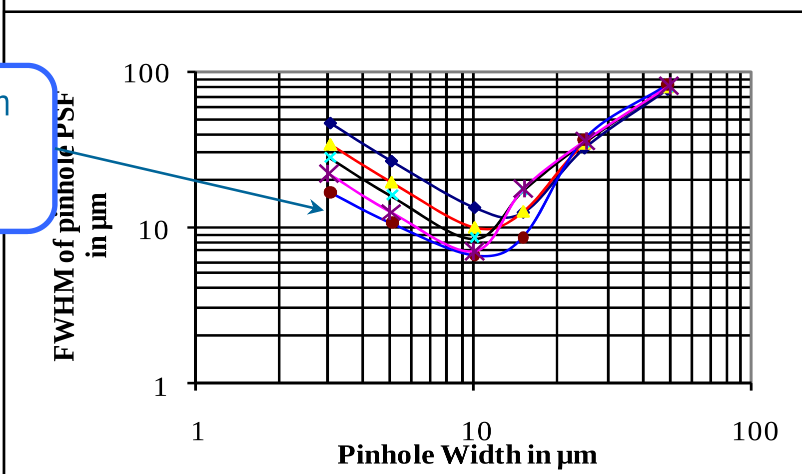

PSF Calculations:

Intensity Distributions at Converter
(White Beam after 1 mm Cu Attenuator)

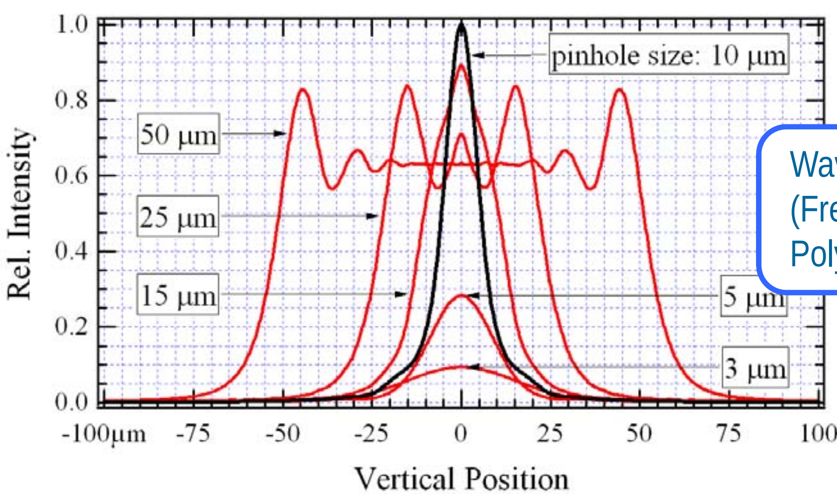

E-Beam Imaging Using **Vertically** Polarized BM SR

Simplified Optical Scheme

(Top View)

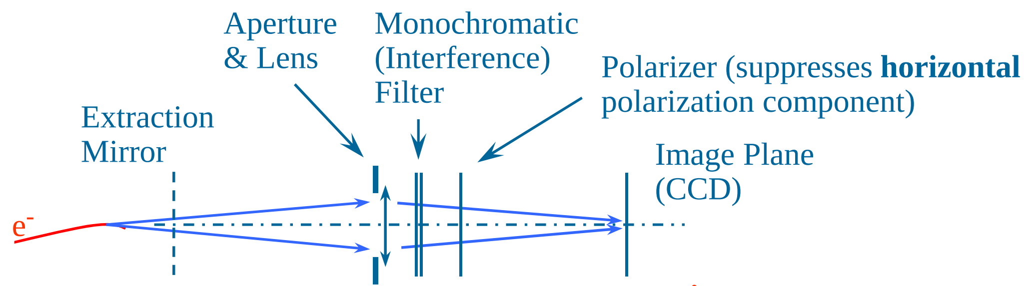

Å.Andersson et.al., Proc. EPAC-96

SR Intensity Distribution in the Image Plane (Vertical Polarization)

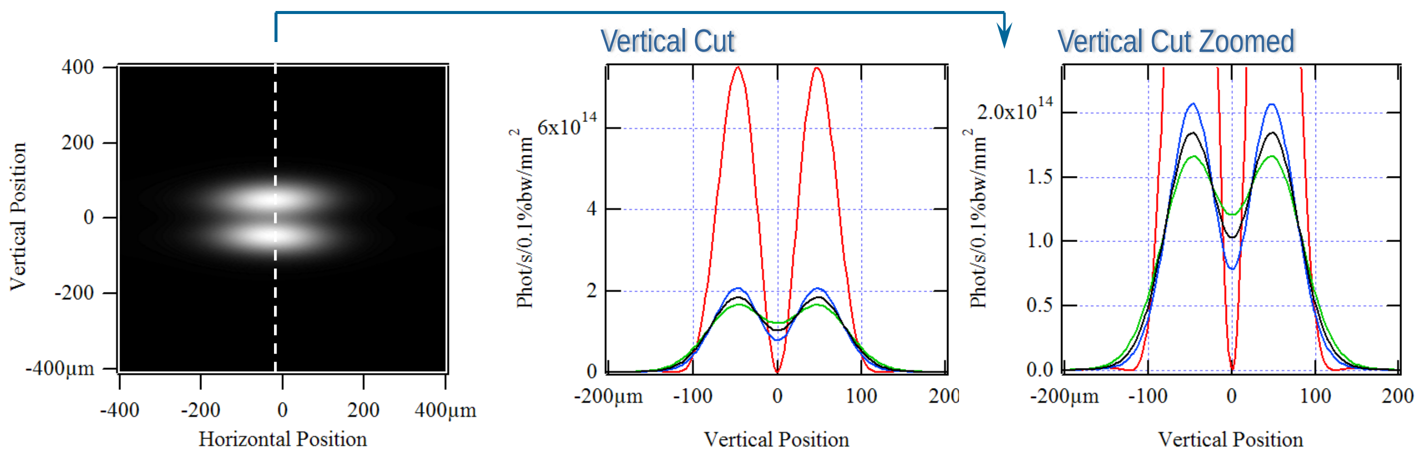

E = 2.75 GeV, I = 500 mA
λ = 500 nm

Optical Magnification: 1
(for simplicity of simulation)

Vert. Angular Aperture: ~12 mr
Hor. Angular Aperture: ~6 mr
(not optimized)

RMS Vertical Size of the E-Beam and the Intensity Fluctuation in the Fringes:

red curve: filament e-beam ($\sigma_{e\,z}$ = 0),	$I_{min}/I_{max} \approx 0$ (< 10^{-3})
blue: $\sigma_{e\,z}$ = 18.3 µm,	$I_{min}/I_{max} \approx 0.36$
black: $\sigma_{e\,z}$ = 23.3 µm (expected),	$I_{min}/I_{max} \approx 0.56$
green: $\sigma_{e\,z}$ = 28.3 µm,	$I_{min}/I_{max} \approx 0.73$

E-Beam Imaging Using Double-Slit Interferometer

Simplified Optical Scheme
(Side View)

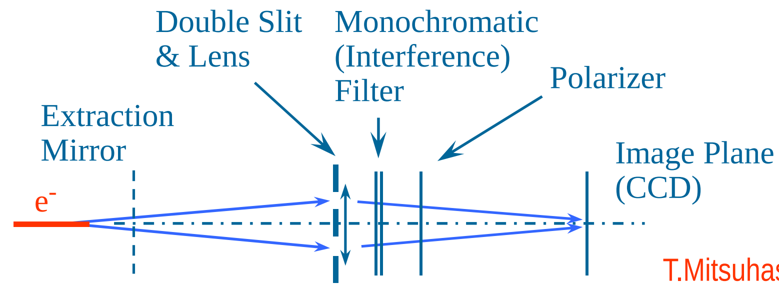

T.Mitsuhashi, Proc. PAC-97

SR Intensity Distribution in the Image Plane (Horizontal Polarization Component)

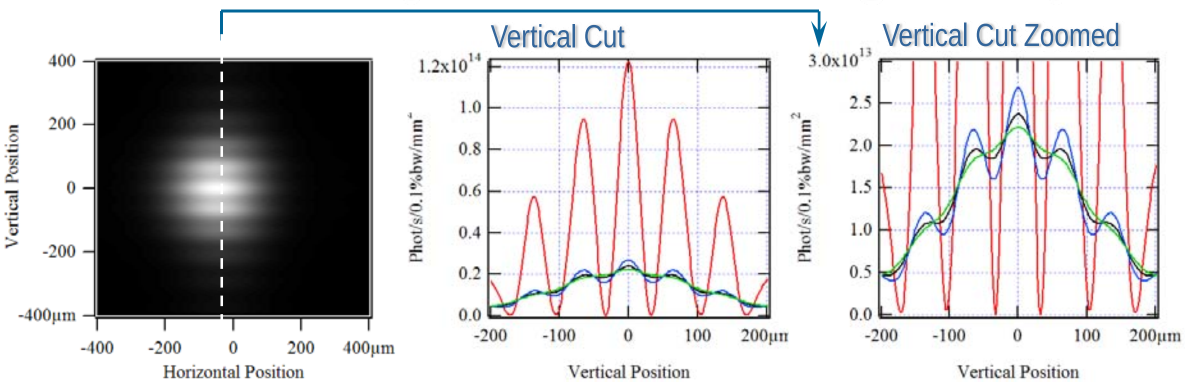

E = 2.75 GeV, I = 500 mA, λ = 500 nm
Distance from Source to Slits: 5 m
Optical Magnification: 1 (for simplicity of simulation)
Vertical Distance between Slits: 30 mm (not optimized)

red: filament e-beam ($\sigma_{e\,z}$ = 0), $I_{min}/I_{max} \approx 0$ ($< 10^{-3}$)
blue: $\sigma_{e\,z}$ = 18.3 μm, $I_{min}/I_{max} \approx 0.59$
black: $\sigma_{e\,z}$ = 23.3 μm, $I_{min}/I_{max} \approx 0.78$
green: $\sigma_{e\,z}$ = 28.3 μm, $I_{min}/I_{max} \approx 0.88$ (no fringes)

SR Intensity Distribution in the Image Plane (Vertical Polarization Component)

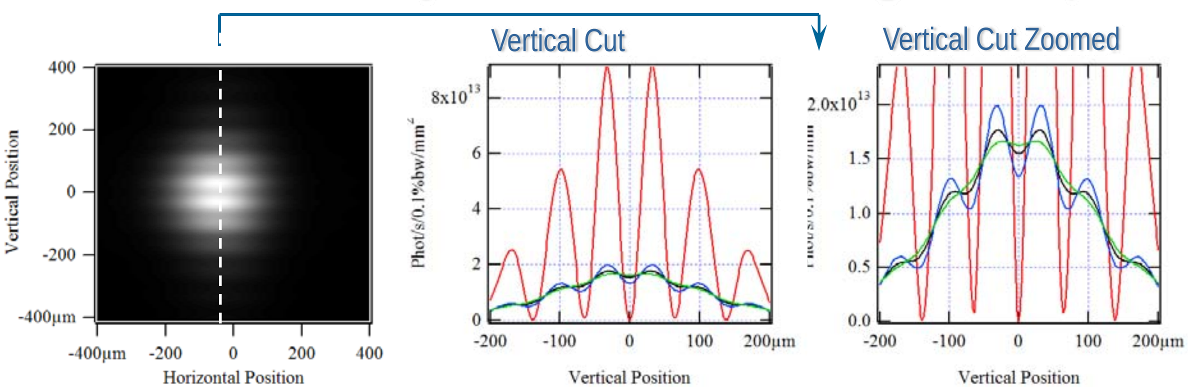

red: filament e-beam ($\sigma_{e\,z}$ = 0), $I_{min}/I_{max} \approx 0$ ($< 10^{-5}$)
blue: $\sigma_{e\,z}$ = 18.3 μm, $I_{min}/I_{max} \approx 0.67$
black: $\sigma_{e\,z}$ = 23.3 μm, $I_{min}/I_{max} \approx 0.88$
green: $\sigma_{e\,z}$ = 28.3 μm, $I_{min}/I_{max} \approx 0.99$ (no fringes)

Angular Horizontal FS Slice Separation Scheme (SLS)

Idea of FS Slicing: A.Zholents (LBNL)

FS Slicing at SLS: G.Ingold et. al.

E-Beam, Modulation:		Radiator:
E_0 = 2.44 GeV	$\Delta E_{max} \approx$ 21.5 MeV	Undulator U19
$I_{s.b.}$ = 2 mA	f_L = 1 kHz	(in-vacuum)
σ_b = 12 ps	σ_L = 21 fs	

Electron Trajectory and Photon Absorbers

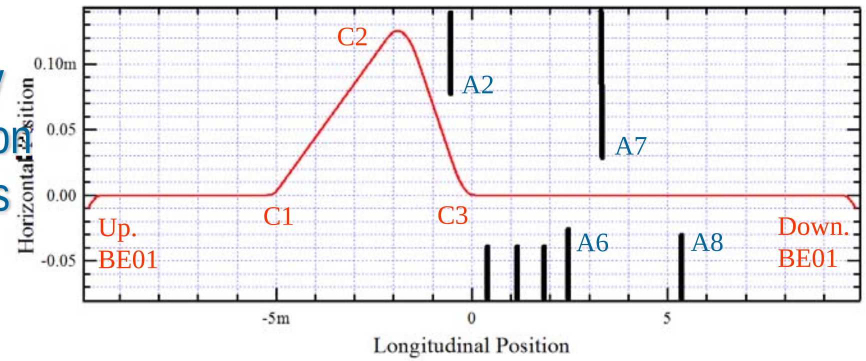

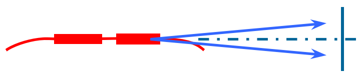

Intensity Distributions in the Median Plane

~15.7 m from Radiator; Finite-Emittance Electron Beam

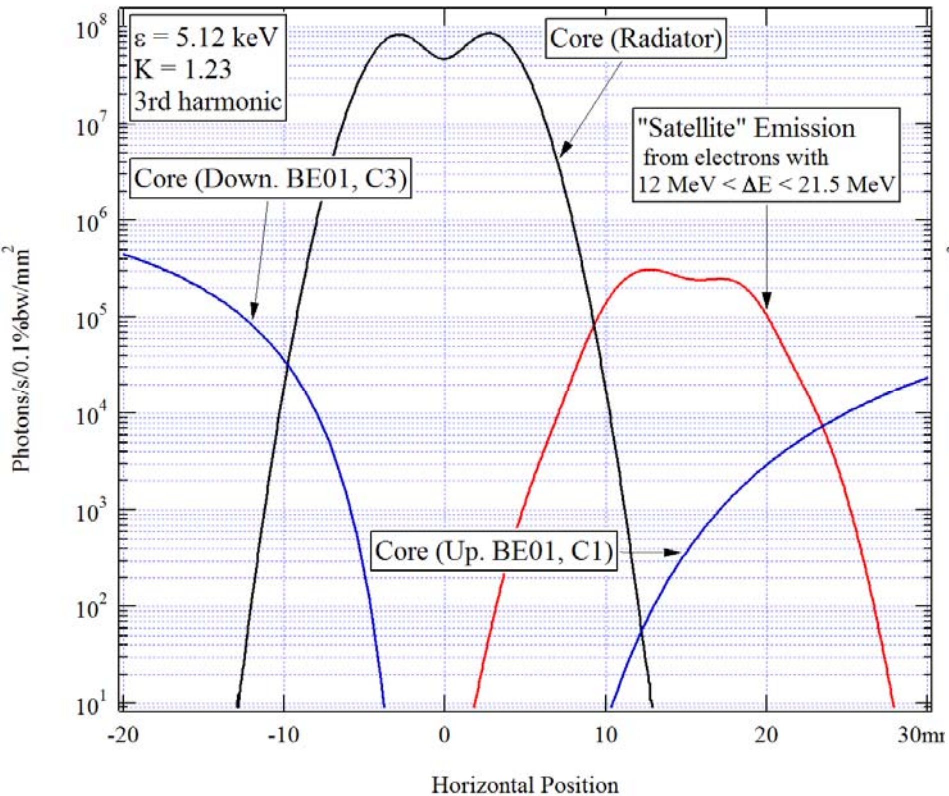

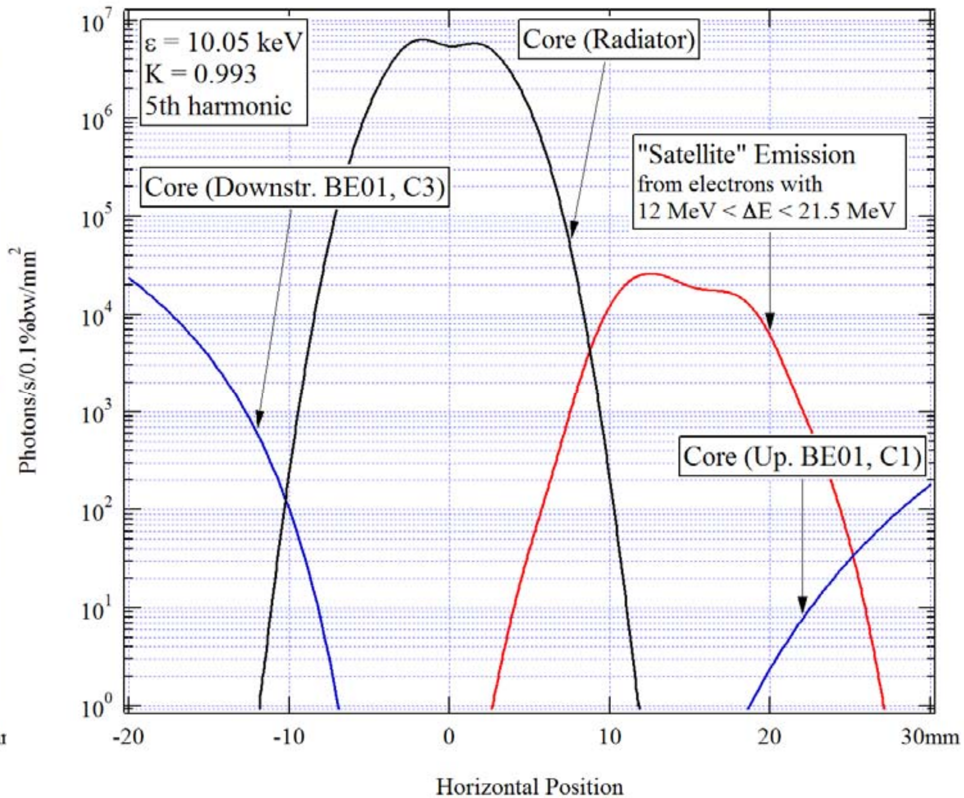

FS Slice Separation Using SOLEIL "Native" Dispersion

Hard X-Rays: Slit- (Pinhole-) Based Spatial Horizontal Separation Scheme

E-Beam, Modulation:

E_0 = 2.75 GeV
$I_{s.b.}$ = 10 mA
σ_b = 24 ps

$\Delta E_{max} \approx$ 14 MeV (pessimistic)
f_L = 10 kHz
σ_L = 50 fs

Hard X-Ray Radiator:

Undulator U20

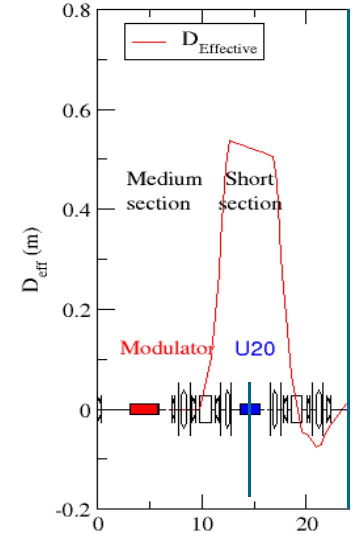

A. Nadji et. al.

$\Delta t_{s\ 7-14\,\mathrm{MeV}} \approx 60$ fs

T. Moreno
M. Idir

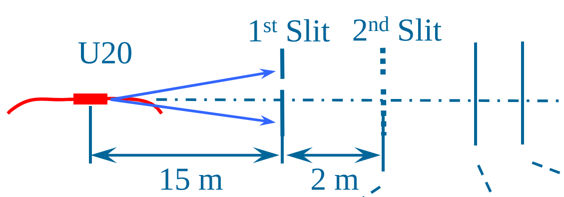

Slit Dimensions:
0.5 mm x 0.5 mm
$|x_c|$ = 2.4 mm

Electron Beam Emittance,
Peculiarities of Undulator Radiation,
Slit Diffraction
are taken into account

Intensity in Transverse Planes After Slit(s)

Cuts by Median Plane

ε = 6.93 keV

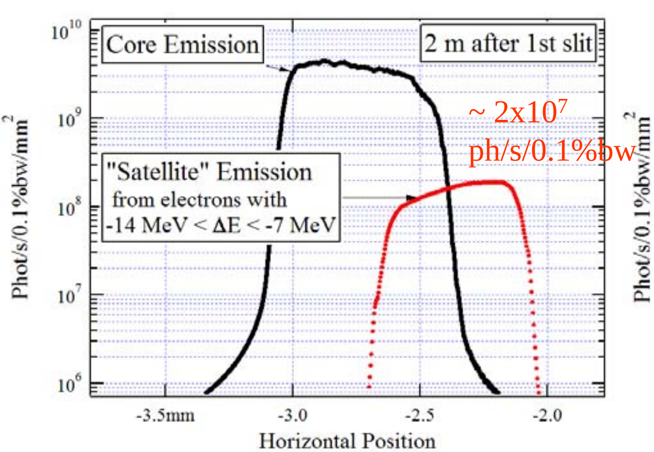

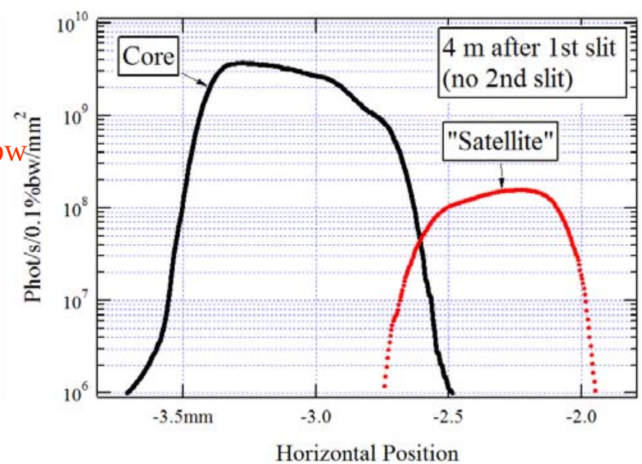

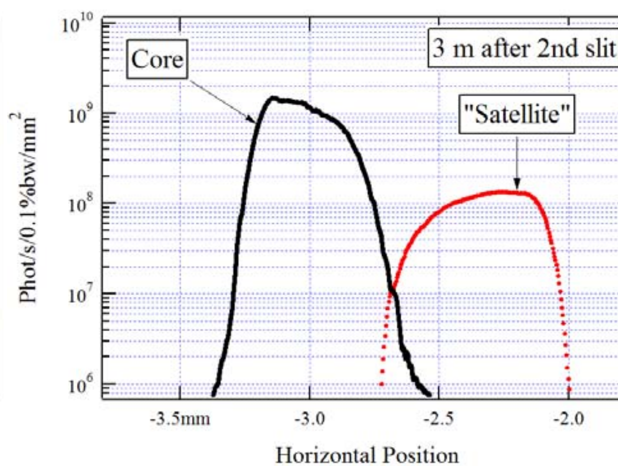

FS Slice Separation Using SOLEIL "Native" Dispersion

Soft X-Rays: Mixed Angular-Spatial Horizontal Separation Scheme

E-Beam, Modulation:

E_0 = 2.75 GeV $\Delta E_{max} \approx$ 20 MeV
$I_{s.b.}$ = 10 mA f_L = 10 kHz
σ_b = 24 ps σ_L = 50 fs

Soft X-Ray Radiator:

Undulator HU80
(Apple-II)

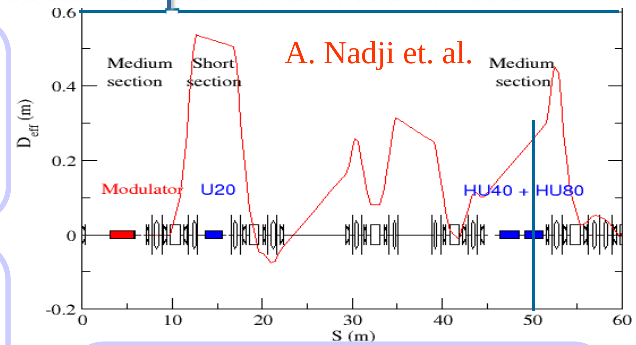

F. Polack

~10 m Slit, Mirror Plane of 1:1 Imaging

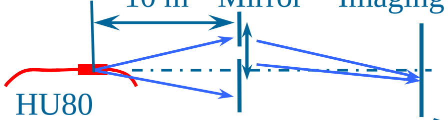

HU80
Centered at
+1.35 m from
the Middle of
Straight Sect.

Slit Dimensions:
2 mm x 1 mm
Slit Position:
$|x_c|$= 2.5 mm

Mirror Surface Assumptions:

- *Average Slope Error: ~1.5 µrad,*
- *Average Roughness: ~ 2.5 Å,*
- *Incidence Angle: ~1°*
- *Error Distribution: Random (Density to be studied)*

- *Peculiarities of Undulator Radiation,*
- *Electron Beam Emittance,*
- *Slit Diffraction,*
- *Scattering from Mirror Surface*

are taken into account

Intensity in Transverse Plane Before Mirror

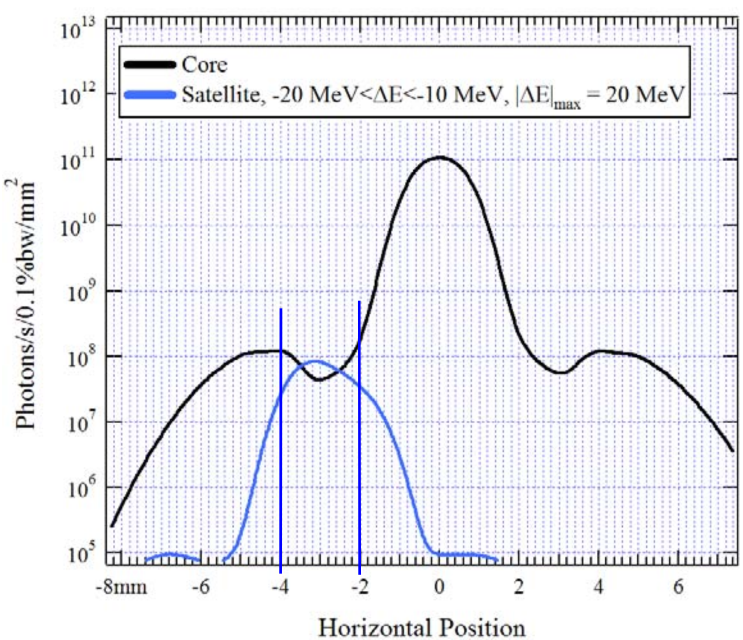

ε = 415 eV

Linear-Horizontal Polarization

$\Delta t_{s\ 10-20\,\mathrm{MeV}} = 180\ \mathrm{fs}$

Intensity in the Plane of 1:1 Imaging

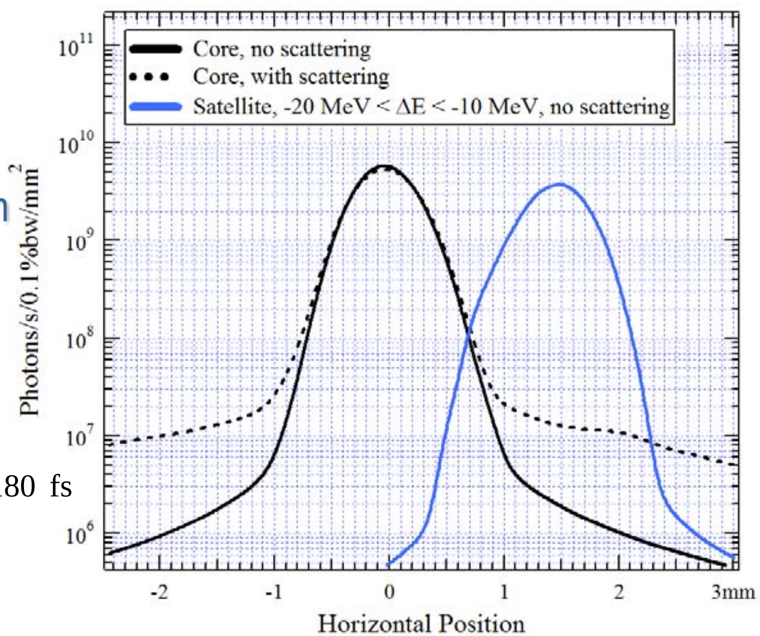

Examples: Infrared Edge Radiation
Emission at Different Wavelengths (SOLEIL)

Magnetic Field (Medium-Size Straight Section)

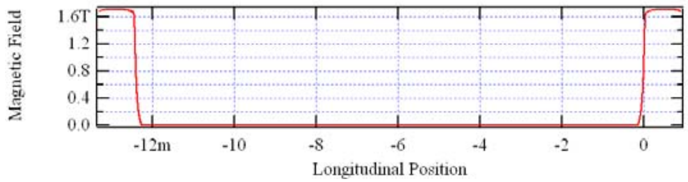

Spectral Flux / Surface (Distance from BM Edge: 1.27 m)

λ = 10 μm

λ = 100 μm

λ = 300 μm

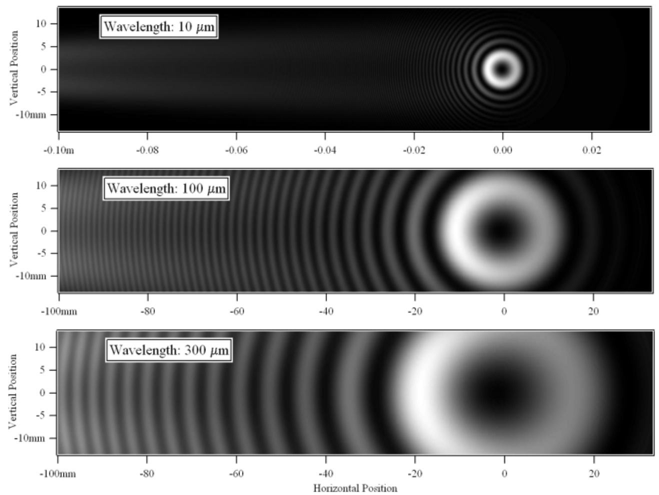

Spectral Flux through Finite Aperture
66.2 mr (= 61 mr + 5.2 mr) Hor. x 18 mr Vert

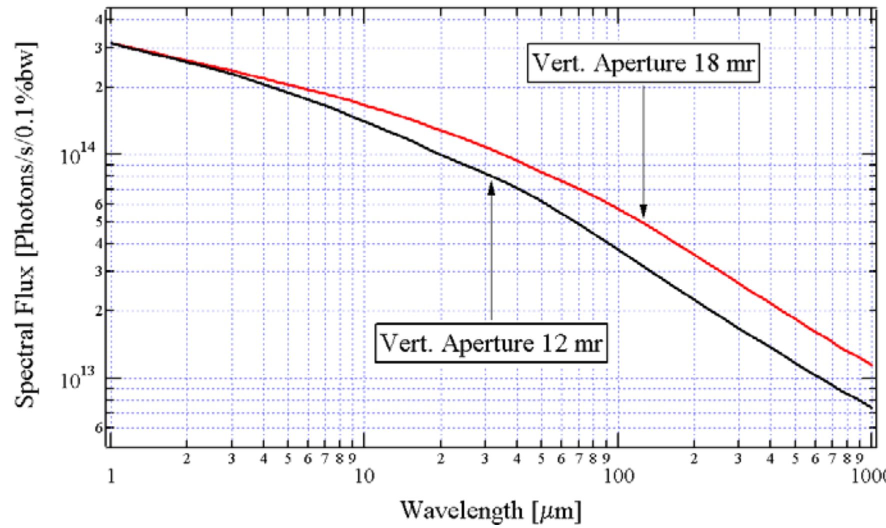

Horizontal Cuts (Median Plane)

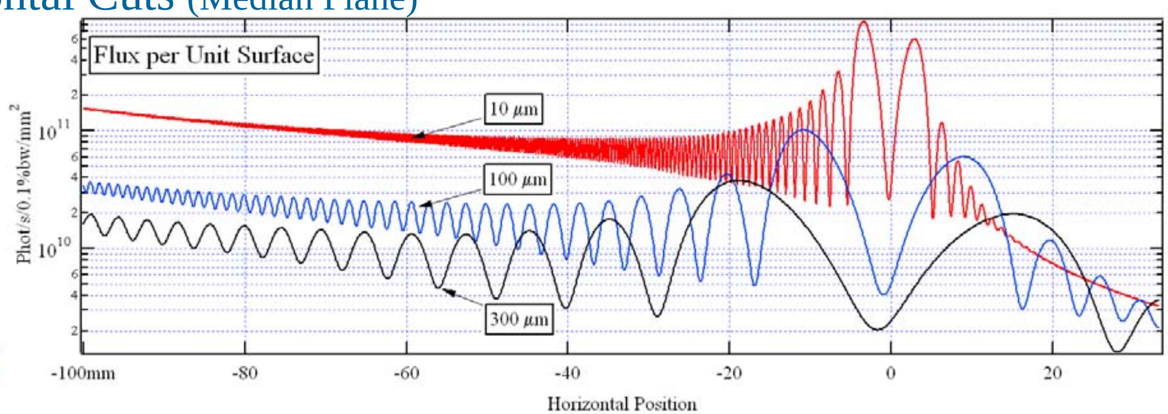

SOLEIL SYNCHROTRON

Examples: Wavefront Propagation

IR1 Extraction Scheme at SOLEIL

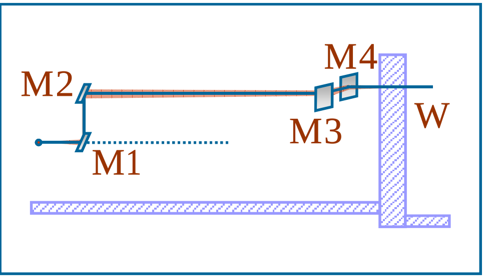

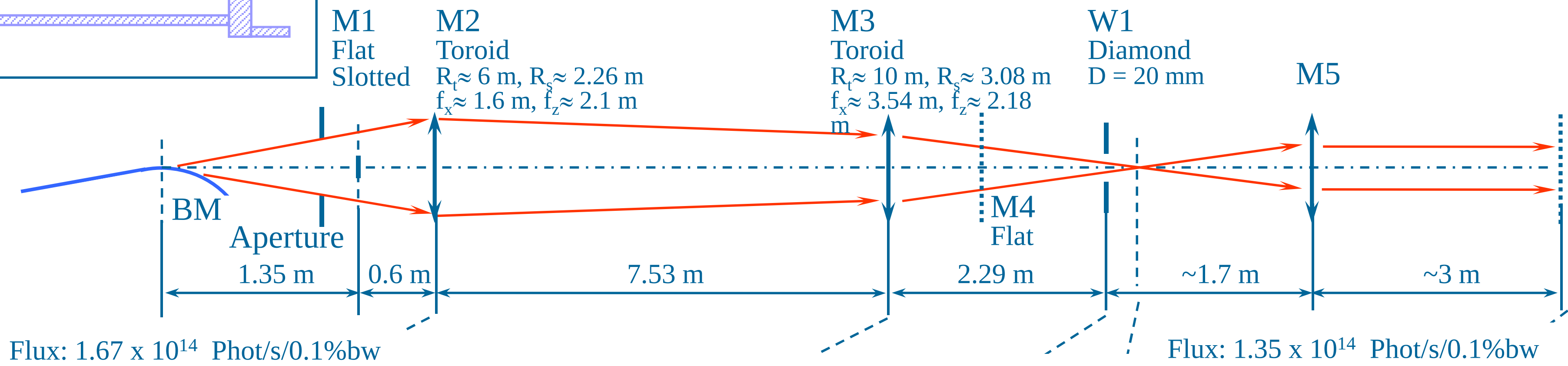

Intensity Distributions at 10 µm Wavelength

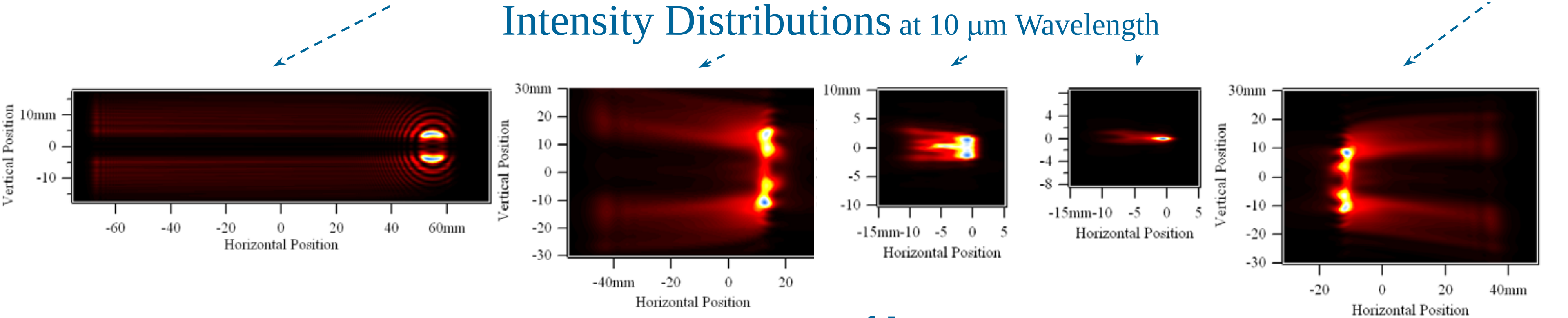

Intensity Profiles

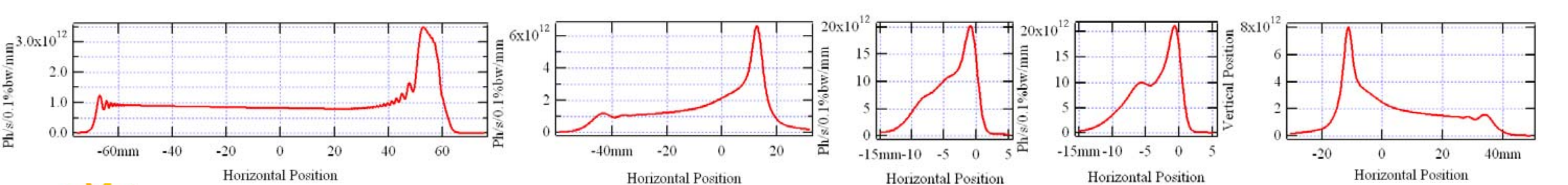

SOLEIL SYNCHROTRON

Optical scheme: F. Polack, P. Dumas

Examples: Time-Dependent Wavefront Propagation

SASE Pulse Profiles and Spectra at FEL Exit

E-Beam: E = 1 GeV $\sigma_{t\,e}$ ~ 200 fs
I_{peak} = 1.5 kA $\varepsilon_x = \varepsilon_y = 1.2\ \pi$ mm-mrad

Undulator: K ~ 2.06
λ_u = 30 mm
L_{tot} ~ 5 x 2 m

ArcEnCiel (phase 2)

A: Seeded FEL operation

$P_{max\ ssed}$ ~ 50 kW
$\sigma_{t\ seed}$ ~ 25 fs

$\hbar\omega_0$ = 100.15 eV

GENESIS

Peak Power vs Long. Position

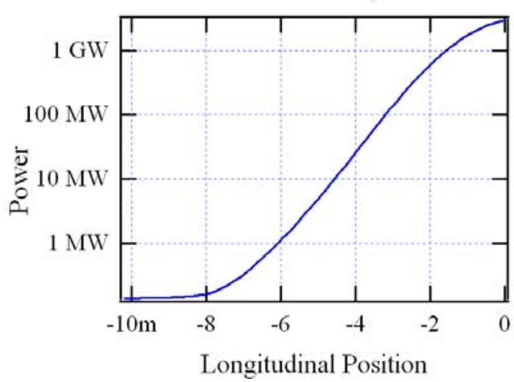

Power vs Time

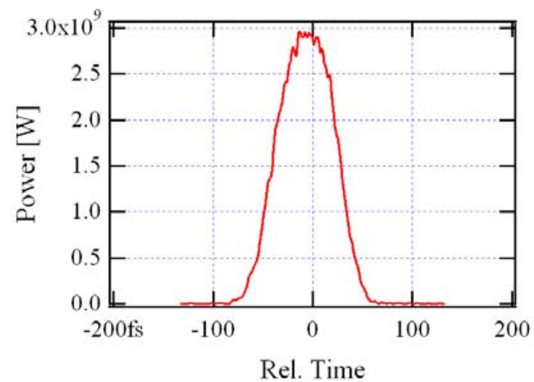

Energy Spectrum

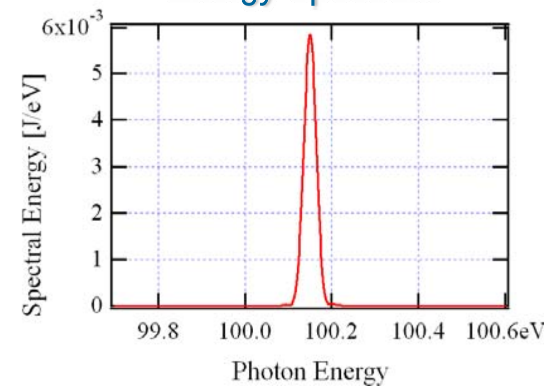

B: SASE (not saturated)

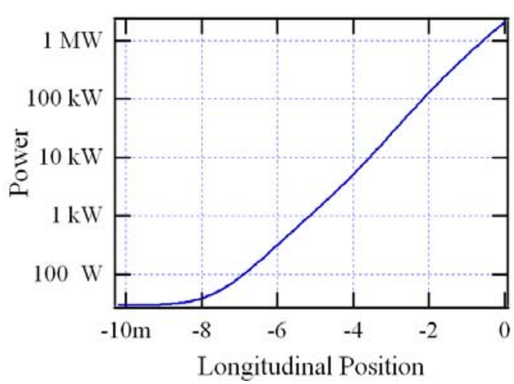

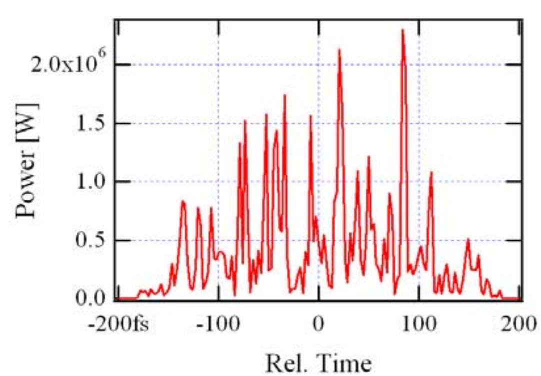

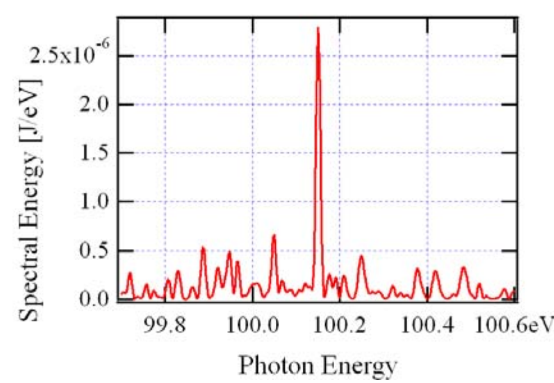

Examples: Time-Dependent Wavefront Propagation

Wavefront Characteristics in Image Plane of Young's 2-Slit Interferometer

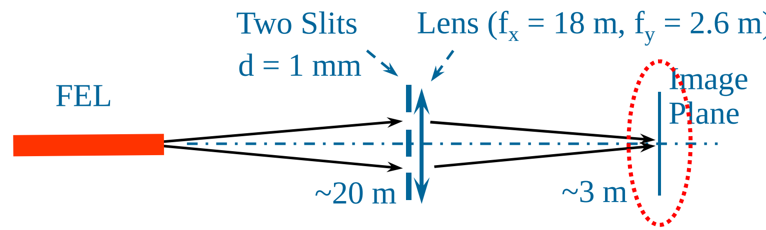

A: Seeded

Spectral Fluence
vs Photon Energy
and Vertical Position (at x = 0)

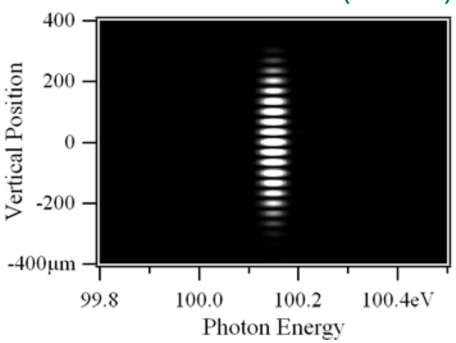

Power Density
vs Time
and Vertical Position (at x = 0)

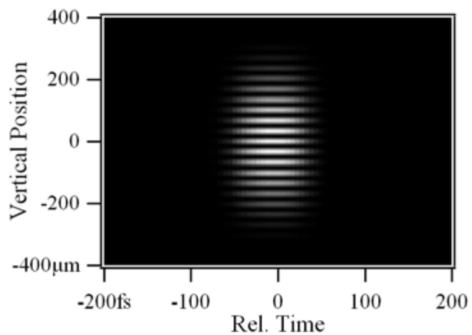

Fluence (/Time-Integrated Intensity)

vs Horiz. and Vert. Positions

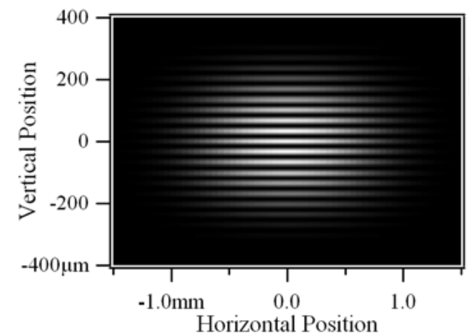

vs Vert. Position (at x = 0)

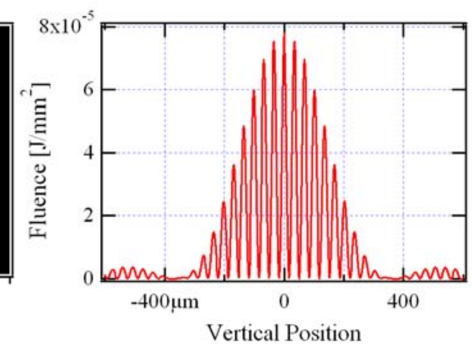

B: Started from noise

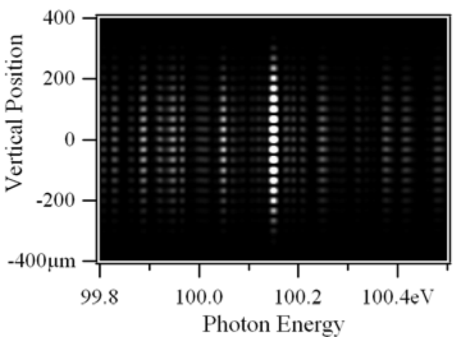

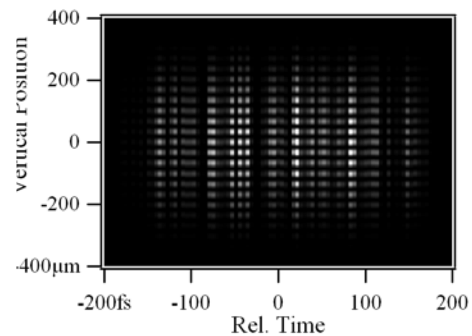

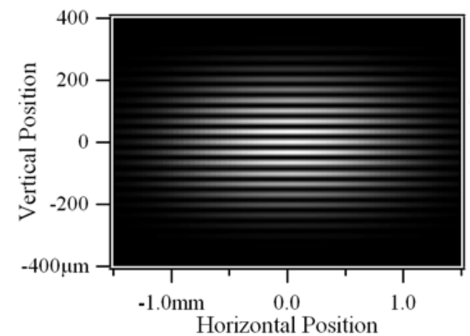

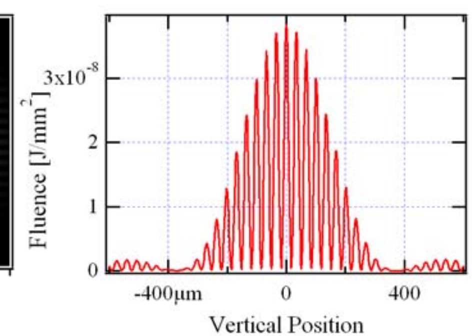

Examples: Time-Dependent Wavefront Propagation

Wavefront Characteristics in Image Plane of a 2-Slit Interferometer with Grating

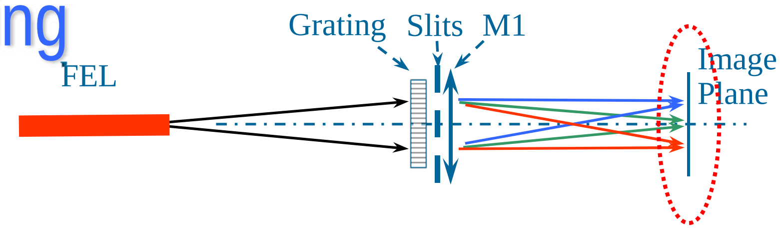

A: Seeded

Spectral Fluence
vs Photon Energy
and Vertical Position (at x = 0)

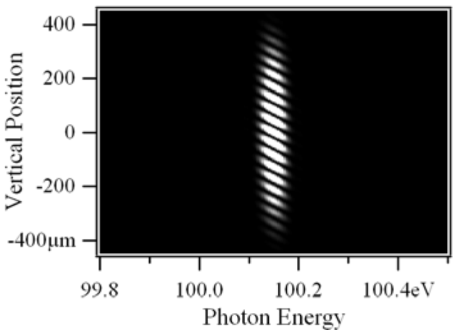

Power Density
vs Time and Vert. Pos. (at x = 0)

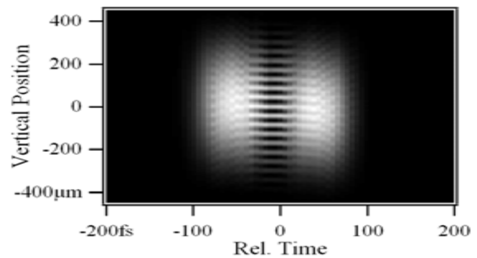

Power vs Time

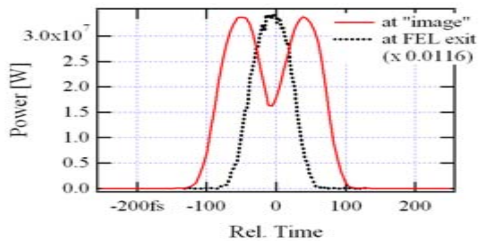

Fluence (/Time-Integrated Intensity)
vs Horiz. and Vert. Positions

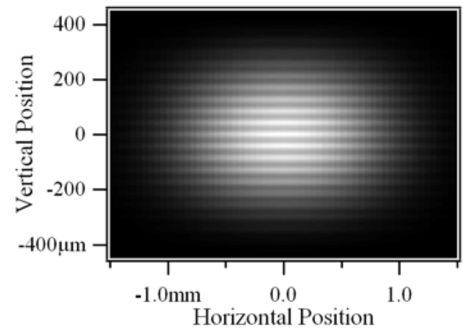

vs Vert. Position (at x = 0)

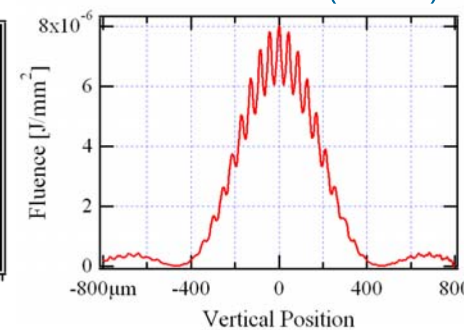

B: Started from noise

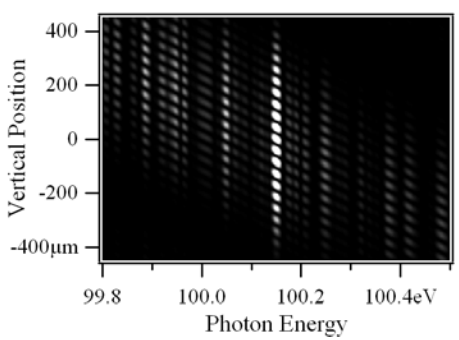

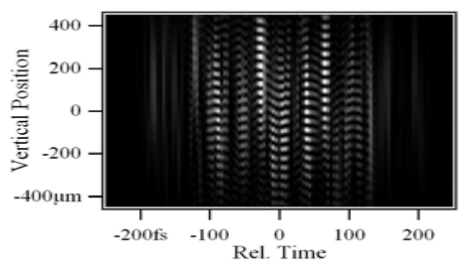

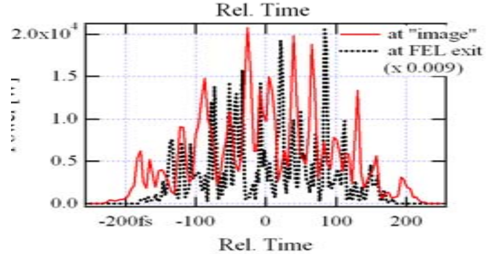

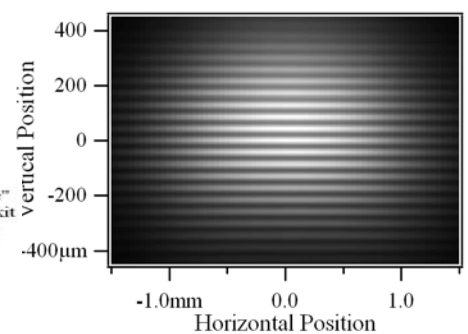

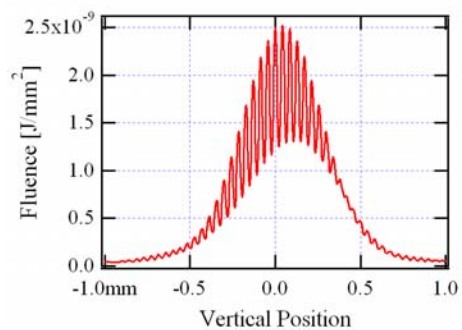

SRW and Others…

RADIA

- Solver of 3D Magnetostatics problems;
- Very efficient for IDs, good for Accelerator Magnets;
- Extension to Eddy Currents is considered

IDBuilder

- GA-based Optimizer for ID construction: magnet Sorting, Swapping, Shimming,…;
- Can be generalized to Magnet Design problems

SRW

- Simulator for Spontaneous Synchrotron Emission and Wavefront Propagation;
- Applicable to large variety of problems of high importance for 3rd and 4th Generation Sources;
- ...However, it is not a “proven” tool for SR Beamline optimization... (yet ?)

- The codes are written in C++ as shared libraries (with documented API);
- Currently interfaced to IGOR Pro (all) and Mathematica (some);
- Can be interfaced to other Front-Ends / Scripting Environments, e.g. Python;
- Are easily “extendable” by users, thanks to Scripting Environments.

Acknowledgements

- J.-L. Laclare, P. Elleaume, J. Chavanne (ESRF)
- J.-M. Filhol, P. Dumas, P. Roy, O. Rudenko (SOLEIL)
- G.P. Williams (JLab), Y.-L. Mathis (ANKA)
- B. Diviacco (ELETTRA), R. Carr (LCLS)
- T. Tanabe, G. Rakowsky (BNL)
- All Users of SRW and RADIA